Optimization on manifolds: A symplectic approach

Guilherme França,[1,*] Alessandro Barp,[2,†] Mark Girolami[2] and Michael I. Jordan[1]

[1]*University of California, Berkeley, USA*

[2]*University of Cambridge, UK*

[*]guifranca@gmail.com, [†]ab2286@cam.ac.uk

Abstract

There has been great interest in using tools from dynamical systems and numerical analysis of differential equations to understand and construct new optimization methods. In particular, recently a new paradigm has emerged that applies ideas from mechanics and geometric integration to obtain accelerated optimization methods on Euclidean spaces. This has important consequences given that accelerated methods are the workhorses behind many machine learning applications. In this paper we build upon these advances and propose a framework for dissipative and constrained Hamiltonian systems that is suitable for solving optimization problems on arbitrary smooth manifolds. Importantly, this allows us to leverage the well-established theory of symplectic integration to derive "rate-matching" dissipative integrators. This brings a new perspective to optimization on manifolds whereby convergence guarantees follow by construction from classical arguments in symplectic geometry and backward error analysis. Moreover, we construct two dissipative generalizations of leapfrog that are straightforward to implement: one for Lie groups and homogeneous spaces, that relies on the tractable geodesic flow or a retraction thereof, and the other for constrained submanifolds that is based on a dissipative generalization of the famous RATTLE integrator.

Contents

1 Introduction

We are concerned with the optimization problem

$$\min_{q \in \mathcal{Q}} f(q), \tag{1.1}$$

where $\mathcal{Q}$ is a smooth manifold—called a *configuration manifold*—and f is smooth. Optimization problems on manifolds have several important applications in machine learning, statistics, and applied mathematics, including maxcut problems, phase retrieval, linear and nonlinear eigenvalue problems, principal component analysis, clustering, and dimensionality reduction, to name a few. In particular, configuration manifolds arise in the context of rank and orthogonality constraints, leading to nonconvex optimization problems. Such problems also appear in statistical physics, e.g., in finding ground states of disordered systems such as spin glasses.

Usually the geometry of $\mathcal{Q}$ is specified by a Riemannian metric that assigns at each point $q \in \mathcal{Q}$ an inner product, $g(q) : T_q\mathcal{Q} \times T_q\mathcal{Q} \to \mathbb{R}$, on the tangent space $T_q\mathcal{Q}$. We are interested in two important classes of manifolds. One is defined through a set of independent constraints, $\psi_a : \mathcal{M} \to \mathbb{R}$, satisfying

$$\psi_a(q) = 0, \qquad a = 1, \ldots, m. \tag{1.2}$$

In this case $\mathcal{Q}$ is a $(n-m)$-dimensional level set embedded into the higher n-dimensional manifold $\mathcal{M}$; i.e., $\mathcal{Q} \equiv \{q \in \mathcal{M} \mid \psi(q) = 0\}$ where $\psi(q) \equiv [\psi_1(q), \ldots, \psi_m(q)]$. See Fig. 1 for an illustration. The geometric properties of $\mathcal{Q}$, in particular its Riemannian metric, are then induced by $\mathcal{M}$—which is usually a Euclidean space although it can be a general smooth manifold. The other main class of manifolds that we are interested in consists of Lie groups and homogeneous spaces where the Riemannian geometry is induced by an inner product on its associated Lie algebra.

We shall adopt a different—and in some sense complementary—approach than that traditionally found in the optimization literature; see, e.g., [1–5] and references therein. The standard approach to optimization on manifolds relies on the Riemannian geometry of $\mathcal{Q}$ and employs the geodesic or gradient flows to obtain optimization schemes. Such an approach is valid once a Riemannian metric has been specified and requires approximating the geodesic flow. It is worth noticing, however, that this can only be done for a handful of manifolds with invariant Riemannian metrics. The dynamics and the underlying geodesic computations take place on the tangent bundle $T\mathcal{Q}$.

Geodesic flows can be seen as Hamiltonian flows over a manifold. More generally, the canonical way to define a dynamical system associated to an arbitrary smooth manifold $\mathcal{Q}$ is through its *cotangent bundle* $T^*\mathcal{Q}$ (see again Fig. 1). The reason is that the cotangent bundle of any smooth manifold is itself a *symplectic manifold* and any dynamics that preserves its symplectic structure is, at least locally, necessarily a Hamiltonian flow. From this perspective, the natural way to approach problem (1.1) is through a *dissipative* Hamiltonian dynamics on $T^*\mathcal{Q}$ where f plays the role of an external potential; dissipation is necessary so that the phase space contracts to a point that corresponds to a solution of the optimization problem (1.1). Relationships between Hamiltonian systems and optimization algorithms on Euclidean spaces has recently seen an explosion of research; see, e.g., [6–12]. In particular, Ref. [8] proposes a general framework that transfers analysis and design tools from conservative to dissipative settings. Herein we will further
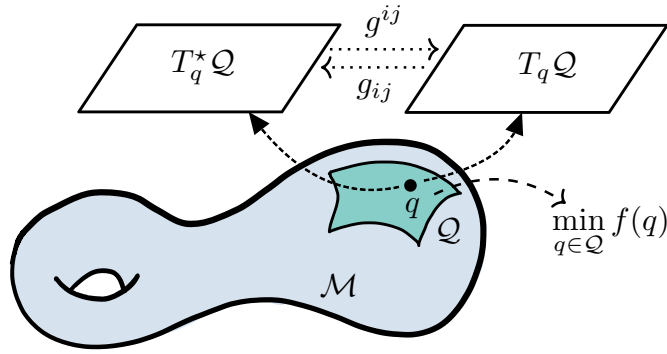
Figure 1: $\mathcal{M}$ is a smooth manifold and $\mathcal{Q} \subset \mathcal{M}$ is a submanifold where the constraints (1.2) are imposed. To every point q we have the tangent space $T_q\mathcal{Q} \subset T_q\mathcal{M}$ and the cotangent space $T_q^*\mathcal{Q} \subset T_q^*\mathcal{Q}$ (which is a symplectic manifold); the tangent bundle $T\mathcal{Q}$ and the cotangent bundle $T^*\mathcal{Q}$ are the respective collections of these spaces over all points $q \in \mathcal{Q}$. A constrained Hamiltonian dynamics is defined on $T^*\mathcal{Q}$ and preserves the geometry of this space. When $\mathcal{M}$ (and thus $\mathcal{Q}$) is a Riemannian manifold there is an isomorphism $T_q\mathcal{M} \cong T_q^*\mathcal{M}$ through the metric g.

extend this approach to arbitrary manifolds and for systems with constraints. In particular, this will allow us to solve problem (1.1) even when the configuration manifold is only implicitly defined; i.e., we do not even need to know the Riemannian metric of $\mathcal{Q}$.

It has long been known that finding accurate long-term numerical approximations of a dynamical flow of interest is usually a challenging, if not hopeless, problem. Importantly, it is not always the problem that one should attempt to solve, a realization that led to the theory of geometric integrators. In this theory the goal is to identify critical properties of the dynamics and to preserve these properties under discretization [13–16]. Examples of such desiderata include conservation of energy, measures, or symmetries, decay of a Lyapunov function, and preservation of a symplectic, Poisson or contact structure. The theory of symplectic integrators, and in particular that of variational integrators (i.e., discrete Lagrangian mechanics), plays a prominent role in the simulation of conservative Hamiltonian systems since such integrators not only preserve the symplectic structure and phase space volume but also the energy up to a bounded error (and in many cases they preserve symmetries of the Hamiltonian as well). Such methods are numerically stable and extremely efficient in practice [17].

Our strategy in this paper involves adapting the theory of symplectic integrators to the dissipative and constrained case via symplectification and splitting procedures. Our point of departure is the framework recently proposed in [8], which applies to the Euclidean case and has been shown to be competive with widely used accelerated methods in that setting. We extend the framework to arbitrary smooth manifolds, and thereby to a significantly wider range of potential applications, including problems not only in machine learning and optimization, but also in molecular dynamics, control theory, complex systems, and statistical mechanics more generally. Our approach provides a first principles derivation—based on symplectic geometry and backward error analysis—of optimization methods on manifolds that emulate dissipative Hamiltonian systems in that they closely preserve the rates of convergence and have long-term stability via the preservation of a geometric structure.

We organize our work as follows. In Sec. 2 we provide a streamlined introduction to our algorithms in the general setting of constrained submanifolds and Lie groups; we provide a rigorous treatment in the Appendix. In Sec. 3 we construct the symplectification of dissipative Hamiltonian systems with constraints. We start with the conservative case and add extra dimensions to incorporate constraints and the explicit time dependency until reaching a symplectic manifold. The original system can then be recovered by a gauge fixing. In Sec. 3.4 we present a concrete example involving an arbitrary geodesic equation with dissipation, constraints, and a drift. This model is general enough to capture most cases of interest in practice. In Sec. 4 we discuss the construction of presymplectic integrators and state their most important properties for this dissipative constrained setting. In Sec. 5 we provide numerical experiments that illustrate the feasibility of our approach.

2   Algorithms

2.1   Submanifolds defined by level sets

Let us introduce a simple and practical algorithm that solves the optimization problem (1.1) subject to constraints (1.2), which define level sets on the ambient space (see Fig. 1). For simplicity, we assume that the Riemannian metric g of $\mathcal{M}$ is constant—this does not represent a limitation since, thanks to Nash or Whitney embedding theorems, the manifold $\mathcal{Q}$ can always be be embedded into $\mathcal{M} = \mathbb{R}^n$ for a sufficiently large n. Thus, define the projection

$$\mathcal{X}_g(q) \equiv \partial_q \psi(q) g^{-1} \partial_q \psi(q)^T, \quad \mathcal{P}_g(q) \equiv I - \mathcal{X}_g^{-1}(q)\partial_q \psi(q) g^{-1}, \tag{2.1}$$

where $\partial_q \psi$ denotes the Jacobian of ψ. A specific algorithm that can be derived within our framework is specified as follows:

$$p_{\ell+1/2} = \mu \mathcal{P}_g(q_\ell)\big[p_\ell - (h/2)\nabla f(q_\ell)\big], \tag{2.2a}$$

$$\bar{p}_{\ell+1/2} = p_{\ell+1/2} - (h\mu/2)\partial_q \psi(q_\ell)^T \lambda_\ell, \tag{2.2b}$$

$$q_{\ell+1} = q_\ell + h\chi g^{-1}\bar{p}_{\ell+1/2}, \tag{2.2c}$$

$$0 = \psi(q_{\ell+1}), \tag{2.2d}$$

$$p_{\ell+1} = \mathcal{P}_g(q_{\ell+1})\big[\mu \bar{p}_{\ell+1/2} - (h/2)\nabla f(q_{\ell+1})\big], \tag{2.2e}$$

where $\ell = 0, 1, \dots$ is the iteration number, $h > 0$ is the discretization step size, $\mu \in [0, 1]$ is responsible for introducing dissipation, and $\chi \equiv \cosh(-\log \mu)$. (Instead of a constant μ one can also use an adaptive μ_ℓ which would be associated to a time-dependent dissipation term.) Note that q is the position coordinates and p their conjugate momenta. We make a number of remarks regarding this method:

(i) Conveniently, it uses an Euclidean gradient, ∇f, instead of parallel transports or geodesic flows (exponential maps) as required by existing optimization approaches on manifolds [1, 3].

(ii) It operates in the cotangent bundle $T^*\mathcal{Q}$ instead of the tangent bundle $T\mathcal{Q}$. Actually, it simulates a dynamical system parametrized on $T(T^*\mathcal{Q})$; hence, it naturally includes "acceleration" from a geometric standpoint.

(iii) It is designed to always stay on the manifold $\mathcal{Q}$, which is enforced by the nonlinear algebraic equation (2.2d). In principle, this equation can be solved for any smooth manifold $\mathcal{Q}$; note that it does not even require knowing the metric of $\mathcal{Q}$. This equation can be solved with any nonlinear solver (such as Newton or quasi-Newton) and this is how the Lagrange multipliers λ_ℓ's are determined.

(iv) This method is based on a more efficient version of RATTLE [18–20] that first splits the Hamiltonian and only applies RATTLE to the kinetic energy, thus providing a symplectic and robust approximation of the geodesic flow [21–23]; see Appendix C for details. This method can also be easily modified to include a reversibility check as proposed in [24].

(v) We have the freedom to choose a constant (positive definite and symmetric) matrix g that acts as a preconditioner and may improve convergence in optimization. In particular, for the purposes of optimization it is convenient to implement a rescaling, $g \mapsto hg$; this corresponds to a change of variables that effectively redefines the discretization step size [7].

(vi) When $\mu = 1$ (conservative case) it recovers the method of [21–23] which is widely employed in numerical simulations in areas such as molecular dynamics and sampling. Thus, the method (2.2) is a "dissipative" generalization of RATTLE. Moreover, in the absence of constraints it recovers one of the symplectic methods of [8] and can be seen as a dissipative generalization of the leapfrog.

(vii) It is second order accurate and, critically, has a dissipative (shadow) Hamiltonian. As a consequence, it approximately preserves the convergence rates of the underlying dissipative Hamiltonian system.

(viii) The method was designed to solve optimization problems with nonlinear *equality* constraints (1.2). However, it is also suitable when some of the functions are replaced by *inequality* constraints, $\psi_a(q) \leq 0$. In this case, the difficult part of the problem consists precisely in enforcing the boundary since when the minimum lies in the interior the constraints become inactive; i.e., we have an unconstrained optimization problem in the interior region. Therefore, this method can also be easily adapted to solve *trust region problems*.

2.2 Lie groups

Consider a matrix representation of the Lie group $\mathcal{G}$—which is the manifold $\mathcal{Q}$—equipped with a bi-invariant metric. Its Lie algebra $\mathfrak{g}$ is a vector space of matrices and we let $\{T_i\}$ be a orthogonal basis thereof. The "dissipative leapfrog" integrator on Lie groups that we propose is

$$Y_{\ell+1/2} = \mu \left[Y_\ell - (h/2)\mathrm{Tr}\left(\partial_X f(X_\ell) \cdot X_\ell \cdot T_i\right) T_i \right], \tag{2.3a}$$

$$X_{\ell+1} = X_\ell \exp\left(hg^{-1}\chi Y_{\ell+1/2}\right), \tag{2.3b}$$

$$Y_{\ell+1} = \mu Y_{\ell+1/2} - (h/2)\mathrm{Tr}\left(\partial_X f(X_{\ell+1}) \cdot X_{\ell+1} \cdot T_i\right) T_i, \tag{2.3c}$$

where $(\partial_X f)_{ij} \equiv \partial f/\partial X_{ji}$, with X_{ij} denoting the entries of the matrix $X \in \mathcal{G}$ (the dot $\cdot$ and Tr denote the matrix product and trace, respectively), and $Y \in \mathfrak{g}$. As before, $\mu \in [0, 1]$, $\chi = \cosh(-\log\mu)$, $h > 0$, and now $g > 0$ is a constant (not a constant matrix as before); we refer to the Appendix D for the derivation of this method. Note that the "momenta" Y is an element

of the Lie algebra and "exp" is the matrix exponential, which defines a map from the Lie algebra to the Lie group—this exponential can also be replaced by any symplectic approximation such as a Cayley transform.

Importantly, the above integrator may also be applied to naturally reductive homogeneous spaces, which include, for example, Stiefel and Grassmannian manifolds, the space of positive definite matrices (and their complex analogues), projective spaces, and affine spaces. In that case one simply needs to restrict the momentum to a vector space complementary to the Lie algebra of the isotropy group, as discussed in the context of sampling [25].

3 Hamiltonian systems

In this section we construct the geometric formalism behind dissipative Hamiltonian systems subject to constraints and emphasize the symplectification procedure where such systems can be embedded into a higher-dimensional symplectic manifold—this will be important later when considering discretizations. We must assume familiarity with differential geometry and Hamiltonian systems; we thus refer to, e.g., [26, 27] for background or the Appendix of [8] for a quick review.

Definition 3.1 (presymplectic manifold). *Let $\mathcal{M}$ be a smooth manifold of dimension $2n + m$, $m \geq 0$, endowed with a 2-form ω of rank $2n$ which is closed. Then $(\mathcal{M}, \omega)$ is a presymplectic manifold and ω is called a presymplectic form. If $m = 0$ then ω is nondegenerate.*

The nondegeneracy condition means that ω defines an isomorphism between the tangent and cotangent bundles—akin to the musical isomorphisms in pseudo-Riemannian manifolds. Presymplectic manifolds generalize the notion of symplectic manifolds (recovered when $m = 0$). While symplectic manifolds can exist only in even dimensions, presymplectic manifolds can also exist in odd dimensions, in which case the presymplectic form ω is necessarily degenerate and thus noninvertible. As we will discuss in a moment, the phase space of a conservative Hamiltonian system is a symplectic manifold while the phase space of a constrained—as well as a dissipative—Hamiltonian system is a presymplectic manifold; e.g., in Fig. 1, $T_q^*\mathcal{M}$ is a symplectic manifold but $T_q^*\mathcal{Q}$ is a presymplectic manifold. Elegant numerical methods such as symplectic integrators were developed for conservative systems. Their most important properties—preservation of symplectic form, long-term stability, and near energy conservation—rely on the existence of a conservation law. This clearly breaks down in a dissipative setting. However, as recently demonstrated [8], if one is able to "symplectify" the system then it is possible to extend these results to nonconservative settings. Here we will further extend such symplectification procedures to constrained cases.

3.1 Conservative and constrained

The Dirac-Bergmann theory of constrained Hamiltonian systems [28–30] was developed to canonically quantize gauge theories. In this framework, the so-called primary constraints have the form $\psi_a(q, p) = 0$. However, for the purposes of optimization it is natural to consider constraints only on the position coordinates (1.2). Such constraints are imposed by adding

Lagrange multipliers to the original Lagrangian or Hamiltonian. In what follows we shall assume we have an embedding, $T^*\mathcal{Q} \hookrightarrow T^*\mathcal{M}$, and assume that the Hamiltonian of interest $H : T^*\mathcal{Q} \to \mathbb{R}$ is obtained as the restriction of a function $T^*\mathcal{M} \to \mathbb{R}$ that is also denoted by H. Thus, the Hamiltonian motion on $T^*\mathcal{Q}$ is defined as a constrained motion on $T^*\mathcal{M}$ that, as we shall see below, takes the form of a *differential-algebraic* equation. This assumption essentially means that the function to be minimized on $\mathcal{Q}$ is given as a function on the n-dimensional manifold $\mathcal{M}$. Furthermore, we can consider a higher-dimensional space $\bar{\mathcal{M}} \equiv \mathbb{R}^m \times \mathcal{M}$ that includes the Lagrange multipliers as degrees of freedom. Thus, on $T^*\bar{\mathcal{M}}$, we consider the extended Hamiltonian

$$\bar{H}(q, p, \lambda, \pi) \equiv H(q, p) + \lambda^a \psi_a(q), \tag{3.1}$$

where (q, p) are local coordinates on $T^*\mathcal{M}$ (which the reader may think of as $\mathbb{R}^{2n}$). Note that $\lambda \equiv (\lambda^1, \ldots, \lambda^m)$ denote the Lagrange multipliers and we have introduced their conjugate momenta $\pi \equiv (\pi_1, \ldots, \pi_m)$—we are using Einstein's summation convention. We have the standard Hamilton's equations on $T^*\bar{\mathcal{M}}$ with Hamiltonian $\bar{H}$. On the constraint surface the corresponding equations of motion are

$$\dot{q}^i = \frac{\partial H}{\partial p_i}, \qquad \dot{p}_i = -\frac{\partial H}{\partial q^i} - \lambda^a \frac{\partial \psi_a}{\partial q^i}, \qquad \dot{\lambda}^a = 0, \qquad \dot{\pi}_a = \psi_a(q) = 0, \tag{3.2}$$

which is a *differential-algebraic equation* on $T^*\mathcal{M}$. This defines the motion on the submanifold $T^*\mathcal{Q} = T^*\mathcal{M}|_{\psi=0} \subset T^*\mathcal{M}$. Moreover, on $T^*\mathcal{Q}$ the dynamics is described by an *ordinary differential equation* that is obtained by solving for the Lagrange multipliers, i.e., substituting $\lambda^a = \lambda^a(q, p)$ explicitly into (3.2). Geometrically, the motion can be derived via the degenerate Hamilton's equations of the presymplectic 2-form $\bar{\Omega}|_{\psi=0} = \omega = dq^i \wedge dp_i$, obtained by restricting the symplectic form $\bar{\Omega} = dq^i \wedge dp_i + d\lambda^a \wedge d\pi_a$ of $T^*\bar{\mathcal{M}}$ [17]. This shows that the phase space $T^*\mathcal{Q}$ of a conservative and constrained Hamiltonian system is a *presymplectic manifold* (Definition 3.1); we note that this fact has already been emphasized in [31, 32].

3.2 Nonconservative

Nonconservative Hamiltonian systems were discussed in [8] and this is the setting of interest for optimization. Such systems can be described by a time-dependent Hamiltonian, $H = H(t, q, p)$. Hamilton's equations have the standard form, however the conservation law $dH/dt = 0$ is now replaced by

$$\frac{dH}{dt} = \frac{\partial H}{\partial t}, \tag{3.3}$$

which captures the phenomenon of dissipation. Since there are no constraints, $\mathcal{Q} = \mathcal{M}$ (see Fig. 1). The dynamics of these systems can be analyzed by embedding $T^*\mathcal{M}$ into a higher-dimensional symplectic manifold, $T^*\hat{\mathcal{M}}$, where $\hat{\mathcal{M}} \equiv \mathbb{R} \times \mathcal{M}$. Thus, let us promote time to a new coordinate, $q^0 \equiv t$, and also introduce its conjugate momentum p_0. We thus have the Hamiltonian

$$\mathscr{H}(q, p) = \mathscr{H}(q^0, q^1, \ldots, q^n, p_0, p_1, \ldots, p_n). \tag{3.4}$$

Without fixing any degrees of freedom we have Hamilton's equations given by

$$\frac{dq^\mu}{ds} = \frac{\partial \mathscr{H}}{\partial p_\mu}, \qquad \frac{dp_\mu}{ds} = -\frac{\partial \mathscr{H}}{\partial q^\mu}, \tag{3.5}$$

7

where $\mu = 0, 1, \ldots, n$ and the time evolution is now parametrized by s. The phase space of this system is the cotangent bundle $T^*\hat{\mathcal{M}}$. The symplectic form is $\Omega \equiv dq^\mu \wedge dp_\mu$ and $(T^*\hat{\mathcal{M}}, \Omega)$ is a symplectic manifold. Requiring that the vector field $X_{\mathscr{H}}$ matches the vector field X_H of the original nonconservative system yields [8]

$$\mathscr{H}(q^0, \ldots, q^n, p_0, \ldots, p_n) \equiv p_0 + H(q^0, q^1 \ldots, q^n, p_1, \ldots, p_n), \tag{3.6}$$

with $s = q^0 = t$ and $p_0(t) = -H(t)$ (the latter is the Hamiltonian as a function of time, i.e., with the actual trajectories replaced). Thus, Eq. (3.6) represents an embedded hypersurface in $T^*\hat{\mathcal{M}}$ which is the phase space of the nonconservative system. Denoting this hypersurface by Γ we thus have $\Omega\big|_\Gamma = \omega = dq^i \wedge dp_i$, i.e., the symplectic form now has rank $2n$ over a manifold of dimension $2n + 2$ so it is degenerate. We conclude that, as in the conservative constrained case, the phase space of a dissipative Hamiltonian system is a *presymplectic manifold* (Definition 3.1).

3.3 Nonconservative and constrained

We now consider the situation where we have an explicit time-dependent Hamiltonian subject to constraints. Combining the previous cases we introduce the extended Hamiltonian

$$\bar{\mathscr{H}}(q, p, \lambda, \pi) \equiv \mathscr{H}(q, p) + \lambda^a \bar{\psi}_a(q), \tag{3.7}$$

with $\mathscr{H}$ being the Hamiltonian defined in (3.4) which is a function on $T^*\hat{\mathcal{M}}$ (recall that $\hat{\mathcal{M}} \equiv \mathbb{R} \times \mathcal{M}$). Besides the time let us also append the Lagrange multipliers to the base manifold, i.e., we define $\bar{\mathcal{M}} \equiv \mathbb{R} \times \mathbb{R}^m \times \mathcal{M} \equiv \mathbb{R}^m \times \hat{\mathcal{M}}$. Note that in the absence of constraints we have $\bar{\mathcal{M}} = \hat{\mathcal{M}}$, recovering Sec. 3.2, while in the conservative case $\bar{\mathcal{M}} = \mathbb{R}^m \times \mathcal{M}$, recovering Sec. 3.1. Hence the Hamiltonian $\bar{\mathscr{H}} : T^*\bar{\mathcal{M}} \to \mathbb{R}$ absorbs both the explicit time dependency of the nonconservative system and the constraints as degrees of freedom and thus defines a dynamics over the *symplectic manifold* $(\bar{\mathcal{M}}, \bar{\Omega})$ with $\bar{\Omega}$ given by Eq. (3.9) below. As will become clear in the next section through a concrete example, for Hamiltonians of interest the constraint term has the form

$$\bar{\psi}_a(q^0, q^1, \ldots, q^n) \equiv \alpha(q^0)\psi_a(q^1, \ldots, q^n), \tag{3.8}$$

where $q^0 = t$ is the original time variable, ψ_a are the constraints (1.2), and the function $\alpha(q^0) > 0$ accounts for dissipation—note that it does not influence the constraint $\psi = 0$. Without yet fixing any degrees of freedom, the equations of motion are given by standard Hamilton's equations (3.5) with $\bar{\mathscr{H}}$, i.e., the dynamics is defined on the symplectic manifold $T^*\bar{\mathcal{M}}$ (of dimension $2n + 2m + 2$) which carries the symplectic form

$$\bar{\Omega} \equiv \underbrace{dq^i \wedge dp_i}_{\text{conservative}} + \underbrace{d\lambda^a \wedge d\pi_a}_{\text{constrained}} + \underbrace{dq^0 \wedge dp_0}_{\text{dissipative}}. \tag{3.9}$$

We now fix some of the degrees of freedom. Enforcing the constraints, i.e., setting $\pi_a = 0$, yields

$$\frac{dq^\mu}{ds} = \frac{\partial\bar{\mathscr{H}}}{\partial p_\mu}, \quad \frac{dp_\mu}{ds} = -\frac{\partial\bar{\mathscr{H}}}{\partial q^\mu} - \lambda^a\frac{\partial\bar{\psi}_a}{\partial q^\mu}, \quad \frac{d\lambda^a}{ds} = 0, \quad \frac{d\pi_a}{ds} = -\bar{\psi}_a(q) = 0, \tag{3.10}$$

which is a *differential-algebraic equation* (DAE) on $T^*\hat{\mathcal{M}}$. Further fixing $s = q^0 = t$ and $p_0 = -H(t)$ the system is then projected into the hypersurface (3.6)—which is the phase space

8

$T^*\mathcal{M}$—yielding

$$\frac{dq^i}{dt} = \frac{\partial H}{\partial p_i}, \quad \frac{dp_i}{dt} = -\frac{\partial H}{\partial q^i} - \alpha(t)\lambda^a\frac{\partial \psi_a}{\partial q^i}, \quad \psi_a(q) = 0, \tag{3.11}$$

where $H = H(t, q^i, p_i)$. This is again a differential-algebraic equation with $2n$ degrees of freedom which are not all independent. Under mild assumptions (see Eq. (3.15) below) the solution for $\lambda^a = \lambda^a(q, p)$ is unique so that we can finally substitute for the Lagrange multipliers to obtain an *ordinary differential equation* (ODE) on $T^*\mathcal{Q}$ (of dimension $2n - 2m$) associated to the original base manifold $\mathcal{Q}$.

On the surface where the constraints are satisfied the second term in (3.9) vanishes and so does the third term by the gauge fixing implied by (3.6). Thus, the Hamiltonian system (3.7) on $T^*\bar{\mathcal{M}}$ is a symplectification of the original nonconservative and constrained Hamiltonian system on $T^*\mathcal{Q}$. After removing the spurious degrees of freedom the symplectic form becomes $\bar{\Omega}|_{\psi=0,\Gamma} = \omega = dq^i \wedge dp_i$, which is degenerate. Therefore, once again, the phase space $T^*\mathcal{Q}$ is a presymplectic manifold (Definition 3.1). The above symplectification procedure can be summarized as follows (we indicate the respective dimensions of each manifold):

$$
\begin{array}{ccccccc}
\bar{\mathcal{M}}^{n+1+m} & \longrightarrow & T^*\bar{\mathcal{M}}^{2n+2+2m} & \dashrightarrow & \bar{\mathscr{H}}(q^\mu, p_\mu, \lambda^a, \pi_a) & \rightsquigarrow & \text{symplectic (ODE)} \\
\uparrow & & \uparrow & & \downarrow{\scriptstyle \pi_a=0} & & \\
\hat{\mathcal{M}}^{n+1} & \longrightarrow & T^*\hat{\mathcal{M}}^{2n+2} & \dashrightarrow & \mathscr{H}(q^\mu, p_\mu) & \rightsquigarrow & \text{presymplectic (DAE)} \\
\uparrow & & \uparrow & & \downarrow{\scriptstyle s=q^0=t} & & \\
\mathcal{M}^n & \longrightarrow & T^*\mathcal{M}^{2n} & \dashrightarrow & H(t, q^i, p_i) & \rightsquigarrow & \text{presymplectic (DAE)} \\
\uparrow & & \uparrow & & \downarrow{\scriptstyle \lambda^a=\lambda^a(q,p)} & & \\
\mathcal{Q}^{n-m} & \longrightarrow & T^*\mathcal{Q}^{2n-2m} & \dashrightarrow & H(t, q^i, p_i) & \rightsquigarrow & \text{presymplectic (ODE)}
\end{array}
\tag{3.12}
$$

Note that only $T^*\bar{\mathcal{M}}$ is a symplectic manifold—the others are presymplectic manifolds—and from $T^*\hat{\mathcal{M}}$ down the system is restricted to the constraint surface. Viewed from the ambient space, the system stays on such a submanifold due to explicit constraints in the equations of motion (which are DAEs). However, the system can also be described by its intrinsic degrees of freedom on $T^*\mathcal{Q}$, i.e., without reference to Lagrange multipliers or constraint functions (these are ODEs). The motion is uniquely specified provided we can solve for the Lagrange multipliers in terms of (q, p).

From the ambient space perspective, the equations of motion (3.11) depend on λ^a since there are derivatives of ψ_a which may not vanish. We thus have the issue of whether the Lagrange multipliers are uniquely determined. Let us show that this is indeed the case when the constraints satisfy a mild condition. Differentiating with respect to time the last equation of (3.11):

$$0 = \frac{d\psi_a}{dt} = \frac{\partial \psi_a}{\partial q^i}\frac{\partial H}{\partial p_i}. \tag{3.13}$$

These are the so-called *hidden constraints*. Differentiating once more:

$$\alpha\lambda^b\left[\frac{\partial \psi_a}{\partial q^i}\frac{\partial^2 H}{\partial p_i p_j}\frac{\partial \psi_b}{\partial q^j}\right] = \frac{\partial H}{\partial p_i}\frac{\partial^2 \psi_a}{\partial q^i\partial q^j}\frac{\partial H}{\partial p_j} + \frac{\partial \psi_a}{\partial q^i}\left[\frac{\partial^2 H}{\partial p_i\partial q^j}\frac{\partial H}{\partial p_j} + \frac{\partial^2 H}{\partial t\partial p_i} - \frac{\partial^2 H}{\partial p_i\partial p_j}\frac{\partial H}{\partial q^j}\right]. \tag{3.14}$$

9

Denoting the Jacobian matrix by $(\partial_q \psi)_{ai} = \partial \psi_a / \partial q^i$ we conclude that λ^a is uniquely determined as a function of (q, p) provided the matrix

$$\partial_q \psi (\partial_{pp} H) \partial_q \psi^T \tag{3.15}$$

is invertible—this is the case when $\partial_q \psi$ has full rank and the Hessian $\partial_{pp} H$ is invertible in the kernel of $\partial_q \psi$. Thus, we can substitute $\lambda = \lambda(t, q, p)$ obtained from (3.14) into (3.11) and the resulting system of differential equations has a locally unique solution. It is important to note that the initial conditions must be consistent, i.e., $\lambda_0 \equiv \lambda(0, q_0, p_0)$ must obey Eq. (3.14), meaning that if the system starts on the constraint surface then it remains on this submanifold for all times.

As a side comment (that will not be needed in the reminder of the paper), note that one can also write (3.11) in Dirac's framework [30]. Assuming the secondary constraints have been resolved, i.e., included together with the primary constraints, which we now assume to have the more general form $\psi_a(q^i, p_i) \approx 0$,[1] let us define $Q^I \equiv (q^\mu, \lambda^a)$ and $P_I \equiv (p_\mu, \pi_\mu)$ to write the equations of motion in terms of Poisson brackets:

$$\frac{dQ^I}{ds} \approx \{Q^I, \bar{\mathscr{H}}\}, \qquad \frac{dP_I}{ds} \approx \{P_I, \bar{\mathscr{H}}\}, \tag{3.16}$$

with (3.7) and (3.8). Writing these equations back to the original coordinates we obtain:

$$\dot{q}^i \approx \{q^i, H\} + \alpha(t)\lambda^a \{q^i, \psi_a\}, \tag{3.17a}$$

$$\dot{p}_i \approx \{p_i, H\} + \alpha(t)\lambda^a \{p_i, \psi_a\}, \tag{3.17b}$$

where now $s = t$. These are precisely the same as (3.11), except that the second term of (3.17a) yields an additional $\alpha \lambda^a \partial \psi_a / \partial p_i$ due to the more general form of nonholonomic constraints.[2] The Dirac bracket assumes the standard form:

$$\{f, g\}_D \equiv \{f, g\} + \sum_{A,B} \{f, \psi_A\} C^{AB} \{\psi_B, g\}, \tag{3.18}$$

where A, B runs over the second-class[3] constraints, and the matrix $C_{AB} \equiv \{\psi_A, \psi_B\}$ is guaranteed to have an inverse, denoted by C^{AB}—note that (3.18) has the standard form even in this dissipative case thanks to the choice (3.8), i.e., p_0 never appears in f, g, ψ_A and thus $\alpha(q^0)$ can be factored outside the Poisson brackets and cancels out.

3.4 Dissipative geodesic equation with drift and constraints

Given a function f to be minimized, we now construct a concrete Hamiltonian of interest that we shall study in the remaining sections. Let $\mathcal{M}$ be an n-dimensional Riemannian manifold equipped

---

[1]Here we use the standard notation where $\approx$ denotes "weak equality" that holds only on the constraint surface.

[2]Note that it is possible to follow the derivation of algorithm (2.2) in the Appendix and include derivative terms $\partial \psi_a / \partial p_i$ to account for the more general constraints $\psi_a(q^i, p_i) \approx 0$.

[3]Recall that ψ_a is first-class if $\{\psi_a, \psi_b\} \approx 0$ for all other constraints ψ_b, i.e., its vector field is everywhere tangent to the constraint surface (they generate gauge transformations). Otherwise, ψ_a is second-class and should be removed by the Dirac bracket (3.18); this prescription isolates the physical degrees of freedom up to a gauge.

with a metric g. As usual, we denote its components by g_{ij} and the components of its inverse by g^{ij}; we can now use g to lower and raise indices and this establishes an isomorphism between $T\mathcal{Q}$ and $T^*\mathcal{Q}$ (recall Fig. 1). We consider the Lagrangian of a dissipative and constrained system given by

$$\bar{L} \equiv e^{\eta(t)} \left[\frac{1}{2} g_{ij}(q)\dot{q}^i \dot{q}^j - f(q) - \lambda^a \psi_a(q) \right], \tag{3.19}$$

where $\eta(t) \geq 0$ is a function of time that is responsible for introducing dissipation. When $\eta = 0$ this reduces to the Lagrangian of a conservative system, while when $\lambda^a = 0$ the system is unconstrained. The Euler-Lagrange equations yield

$$\ddot{q}^i + \Gamma^i{}_{jk}\dot{q}^j\dot{q}^k + \gamma\dot{q}^i = -g^{ij}\frac{\partial f}{\partial q^j} - g^{ij}\lambda^a\frac{\partial \psi_a}{\partial q^j}, \qquad \psi_a(q) = 0, \tag{3.20}$$

where $\gamma(t) \equiv \dot{\eta}(t)$ and $\Gamma_{ijk}(q) \equiv \frac{1}{2}\left(\partial_k g_{ij} + \partial_j g_{ik} - \partial_i g_{jk}\right)$ are the Christoffel symbols. This is a generalization of the *geodesic equation*, i.e., we have introduced dissipation, constraints, and a drift $\partial_q f$. The standard geodesic equation is recovered when $\gamma = 0$, $\psi_a = 0$, and $f = 0$—and this differential-algebraic equation evolves in the tangent bundle $T\mathcal{M}$.

Let us now move to the cotangent bundle $T^*\mathcal{M}$. The canonical momentum is defined as

$$p_i \equiv \frac{\partial \bar{L}}{\partial \dot{q}^i} = e^{\eta(t)} g_{ij}\dot{q}^j, \tag{3.21}$$

from which we obtain the Hamiltonian:

$$\bar{H} = \frac{1}{2} e^{-\eta(t)} g^{ij}(q) p_i p_j + e^{\eta(t)} \left[f(q) + \lambda^a \psi_a(q) \right]. \tag{3.22}$$

Note that $\alpha(t)$ in (3.8) is simply $e^{\eta(t)}$. We have obtained constrained Hamilton's equations on $T^*\mathcal{M}$:

$$\dot{q}^i = e^{-\eta} g^{ij} p_j, \qquad \dot{p}_i = -\frac{e^{-\eta}}{2}\frac{\partial g^{k\ell}}{\partial q^i} p_k p_\ell - e^{\eta}\frac{\partial f}{\partial q^i} - e^{\eta}\lambda^a\frac{\partial \psi_a}{\partial q^i}, \qquad \psi_a(q) = 0. \tag{3.23}$$

One can check that combining these equations yields precisely (3.20). The (intrinsic) phase space of the system is

$$T^*\mathcal{Q} \equiv T^*\mathcal{M}\big|_{\psi=0} = \left\{ (q,p) \in T^*\mathcal{M} \,|\, \psi(q) = 0, \, \partial_q \psi^T g^{-1} p = 0 \right\}. \tag{3.24}$$

The requirement that g is a Riemannian metric automatically satisfies (3.15) (assuming that $\partial_q \psi$ has full rank).

4 "Rate-matching" geometric integrators

We now state general results for geometric integrators of nonconservative and constrained Hamiltonian systems that generalize classical results for symplectic integration of conservative, unconstrained systems. We are thereby able to construct numerical methods for solving problem (1.1) from first principles.

Definition 4.1 (presymplectic integrator). *A numerical map ϕ_h (with step size $h > 0$) is said to be a* presymplectic integrator *for a constrained and nonconservative Hamiltonian system if it is obtained by reducing (i.e., by gauge fixing) a constrained symplectic integrator with a generating map to its symplectification.*

Critically, the requirement that the integrator has a generating map ensures the existence of a globally defined *shadow Hamiltonian* without any assumption on the topology of the manifold. In particular, splitting methods such as leapfrog and variational integrators such as RATTLE do have a generating map given by a discrete Lagrangian [17].

Concretely, we consider (3.7) which is a conservative system and therefore suitable for the application of a *symplectic* integrator. We then fix $s = t = q^0$ and $p_0 = -H(t)$ to project the system onto the hypersurface (3.4), thus recovering the original degrees of freedom of the nonconservative constrained system. Importantly, p_0 does not participate in the dynamics since it is only a fixed function of time, i.e., p_0 does not couple to the other degrees of freedom and for this reason can be ignored. Moreover, the discretization of q^0 is exact. Thus, the only source of discretization error comes from the (constrained) symplectic integrator applied to the higher-dimensional system. As a consequence, the resulting "dissipative" presymplectic integrator has the same order of accuracy as the conservative symplectic integrator.

Theorem 4.2. *Consider a presymplectic integrator ϕ_h of order r for a constrained and nonconservative Hamiltonian system whose true flow is denoted by φ_t. This method preserves the time-varying Hamiltonian up to a bounded error:*

$$H \circ \phi_\ell^\ell = H \circ \varphi_{t_\ell} + \mathcal{O}(h^r), \tag{4.1}$$

for $t_\ell = h\ell = \mathcal{O}(h^r e^{c/h})$ and some constant $c > 0$.

Proof. Consider the symplectification of the Hamiltonian vector field:

$$X_{\mathscr{H}} = X_{p_0} + X_H = \frac{\partial}{\partial q^0} - \frac{\partial H}{\partial q^0}\frac{\partial}{\partial p_0} + X_H. \tag{4.2}$$

The flow of X_{p_0} is given by

$$\frac{dq^0}{ds} = 1, \qquad \frac{dp_0}{ds} = -\frac{\partial H}{\partial q^0}, \tag{4.3}$$

where s denotes the (new) time parameter. The solution of these equations are

$$q_0(s) = s, \qquad p_0(s) = -H(s) + H(0) + p_0(0) = -H(s) + \mathscr{H}(0), \tag{4.4}$$

provided $q^0(0) = 0$ (which now makes $s = t$). The Hamiltonian is determined up to an arbitrary constant and it is convenient to take $\mathscr{H}(0) = 0$ since then the p_0 coordinate simply corresponds to the value of the Hamiltonian at a given instant of time. Note that these equations are still satisfied along the flow of $X_{\mathscr{H}}$. A presymplectic integrator is, according to Definition 4.1, any symplectic integrator Ψ_h for which q^0, p_0 are integrated exactly (see also [33, 34]). Let us denote $y \equiv (q^\mu, p_\mu)$, $z \equiv (q^i, p_i)$ and $y_\bullet \equiv y(s = 0)$. Thus, requiring $q^0(0) = 0$ we have $q_\ell^0 \equiv (q^0 \circ \Psi_h^\ell)(y_\bullet) = q^0 \circ \Phi_{hl}(y_\bullet) = h\ell$ where Φ_s denotes the true flow of $\mathscr{H}$. Because the

integrator is symplectic and has a generating map—e.g., it is variational integrator such as RATTLE or leapfrog—we have a globally defined shadow Hamiltonian from which it follows that

$$\mathscr{H} \circ \Psi_h^\ell = \mathscr{H} \circ \Phi_{h\ell} + \mathcal{O}(h^r), \tag{4.5}$$

for $s_\ell = \ell h = \mathcal{O}(h^r e^{c/h})$ and some constant $c > 0$. Defining the projection $\pi : \mathbb{R}^2 \times T^*\mathcal{Q} \to \mathbb{R} \times T^*\mathcal{Q}$, $y \mapsto (q^0, z)$, we have $\mathscr{H} = p_0 + H \circ \pi$. Moreover, $\pi \circ \Phi_{h\ell} = \varphi_{h\ell} \circ \pi$ where φ_t is the true flow of the original dissipative Hamiltonian system on $\mathbb{R} \times T^*\mathcal{Q}$. Hence from (4.5) we conclude:

$$p_0 \circ \Psi_h^\ell + H \circ \pi \circ \Psi_h^\ell = p_0 \circ \Phi_{k\ell} + H \circ \varphi_{h\ell} \circ \pi + \mathcal{O}(h^r). \tag{4.6}$$

Since p_0 is integrated exactly, i.e., $p_0 \circ \Psi_h^\ell = p_0 \circ \Phi_{h\ell}$, we obtain

$$H \circ \pi \circ \Psi_h^\ell = H \circ \varphi_{h\ell} \circ \pi + \mathcal{O}(h^r) \tag{4.7}$$

and finally

$$H \circ \phi_h^\ell = H \circ \varphi_{h\ell} + \mathcal{O}(h^r) \tag{4.8}$$

since

$$\phi_h^\ell \circ \pi = \pi \circ \Psi_h^\ell, \tag{4.9}$$

where we recall that ϕ_h is the presymplectic integrator that acts on $\mathbb{R} \times T^*\mathcal{Q}$. $\qquad\square$

This extends the main result of [8] to constrained cases. In general it is impossible to preserve both the symplectic structure and the Hamiltonian [35]. Presymplectic integrators are designed to exactly preserve the presymplectic structure of nonconservative constrained systems; however, they are also guaranteed to preserve the Hamiltonian up to a small error which, importantly, does not grow with time—this is in contrast to most discretizations for which such an error would be unbounded regardless of the order of the integrator.

This argument shows that the value of the dissipative Hamiltonian H along the presymplectic integrator stays close to the true value of the Hamiltonian along the suspension vector field, $\partial_{q^0} + X_H$, whose flow yields the true time-dependent mechanics on $T^*\mathcal{Q}$—note that in the above proof we can replace $T^*\mathcal{Q}$ by any symplectic manifold. Furthermore, from the shadow expansion $\widetilde{\mathscr{H}} = \mathscr{H} + h\mathscr{H}_1 + h^2\mathscr{H}_2 + \cdots$, there exists a *shadow dissipative Hamiltonian* $\widetilde{H}$ given by

$$\widetilde{H} \circ \pi = H \circ \pi + h\mathscr{H}_1 + h^2\mathscr{H}_2 + \cdots. \tag{4.10}$$

In optimization and computer science one is often interested in complexity results. Suppose we have a dissipative system, such as (3.20), where a convergence rate,

$$f(q(t)) - f^\star = \mathcal{O}(\mathcal{R}(t)), \tag{4.11}$$

is known a priori. Here $\mathcal{R}(t)$ is a decreasing function that describes how fast the system approaches a local minimum $f^\star$. As a direct consequence of Theorem 4.2, presymplectic integrators are guaranteed to nearly preserve such rates on arbitrary Riemannian manifolds. To see this, let $\phi_h : T^*\mathcal{Q} \to T^*\mathcal{Q}$ be a presymplectic integrator of order $r \geq 1$. Then there exists a metric d such that [36]

$$d\big(\phi_h^\ell(z_\bullet), \varphi_{t_\ell}(z_\bullet)\big) \leq C_\ell h^r, \tag{4.12}$$

13

where $z_\bullet \equiv (q(0), p(0))$ is the initial state, $t_\ell = h\ell$ is the simulation time, and we recall that φ_t is the true flow of the system. The constant C_ℓ in general grows with ℓ. For instance, on $\mathbb{R}^n$ it is common to use [13]

$$C_\ell = C(e^{L_\phi t_\ell} - 1), \tag{4.13}$$

where L_ϕ is a Lipschitz constant of the integrator and $C > 0$ is an independent constant that does not depend on ℓ. Such a bound holds for the majority of methods, even non-structure-preserving ones. Here we assume this rough bound is also true for (4.12) on the manifold $T^*\mathcal{Q}$. It is now straightforward to show the following.

Corollary 4.3. *Consider the dissipative and constrained geodesic equation* (3.20)—*or equivalently Hamilton's equations* (3.23)—*over a Riemannian manifold $\mathcal{M}$. Suppose a convergence rate* (4.11) *is known. Then a presymplectic integrator of order r preserves this rate up to*

$$f \circ \phi_h^\ell = f \circ \varphi_{h\ell} + \mathcal{O}(h^r e^{-\eta(ht_\ell)}), \tag{4.14}$$

provided $e^{L_\phi - \eta(t)} < \infty$, where L_ϕ is a Lipschitz constant of the numerical integrator, and this holds for exponentially large times $t_\ell = \mathcal{O}(h^r e^{c/h})$.

Proof. Consider the Hamiltonian (3.22), i.e., $\bar{H} = H + \lambda^a \bar{\psi}_a$ where $H = (1/2)e^{-\eta(t)}g^{ij}p_i p_j + e^{\eta(t)}f(q)$ is the original Hamiltonian. Replacing H into (4.1)—note that this already accounts for the constraints—yields

$$f \circ \phi_h^\ell - f \circ \varphi_{h\ell} = e^{-2\eta(t_\ell)} \left(T \circ \varphi_{h\ell} - T \circ \phi_h^\ell \right) + \mathcal{O}(e^{-\eta(t_\ell)}h^r), \tag{4.15}$$

where $T(q,p) \equiv (1/2)p \cdot g^{-1}(q)p$ is the kinetic energy. We have a Lipschitz condition:

$$\left| \left(T \circ \varphi_{h\ell} - T \circ \phi_h^\ell \right)(z_\bullet) \right| \le L_T C(e^{L_\phi t_\ell} - 1)h^r, \tag{4.16}$$

where we have used (4.12) with (4.13). Therefore,

$$\left| f \circ \phi_h^\ell(z) - f \circ \varphi_{h\ell}(z) \right| \le e^{-\eta(t_\ell)}h^r \left[L_T(C/2)(e^{L_\phi t_\ell} - 1)e^{-\eta(t_\ell)} + K \right]. \tag{4.17}$$

The result follows since $e^{L_\phi t_\ell - \eta(t_\ell)}$ is bounded by assumption. $\qquad\square$

Thus, provided the system is suitably dampened (choice of $\eta(t)$) the continuous-time rates will be closely matched on any Riemannian manifold—the error is exponentially small in (4.14). In the Appendix we also provide an alternative argument to Corollary 4.3 by using the symplectified Hamiltonian. Based on the above result one can establish convergence rates of numerical methods by considering a Lyapunov analysis for the continuous system alone.[4]

---

[4]We stress that the focus of this paper is not in establishing such continuous-time rates but rather in providing a general framework that ensures that such rates—whatever they are—are closely preserved in discrete time.

4.1 Why presymplectic integrators?

Purely from the point of view of optimization, there is no necessary reason for employing a geometric integrator. Indeed, from the proof of Corollary 4.3 we see that the key ingredient relevant to numerical methods is that the geometric integrator preserves the Hamiltonian within a bounded error. This condition can, however, be ensured by other types of discretization as well, e.g., by constructing methods based on energy-preserving integrators. In this case the Hamiltonian would be exactly preserved and the rates would be matched even more directly (i.e., the constant K would be absent from inequality (4.17)). Another approach would be to construct methods that exactly preserve a Lyapunov function, assuming one is known. While these approaches would be sufficient to obtain "rate-matching" discretizations, there are other desirable numerical consequences that derive from the use of geometric integrators.

It is important to note that in general it is impossible to preserve both the energy and the symplectic structure [35]. Symplectic integrators exactly preserve the former and as a consequence they also nearly preserve the latter. Thus, the geometric integrators we have constructed for the dissipative case inherit the Hamiltonian structure of the system, implying that the numerical trajectories stay on the the manifold of interest; this is particularly important for optimization on manifolds. In contrast, the majority of other discretizations will move away from the manifold and necessitate some type of projection back to the manifold. Unfortunately, such projections can only be computed in very few special cases. Moreover, the constraint formulation we have presented is quite versatile since it allows one to solve problems on manifolds that are only implicitly defined, e.g., manifolds that can be immersed in $\mathbb{R}^n$.

Another advantage of our geometric integrators is that they are simple to implement—they only require standard gradient computations of the objective function and, in the constrained case, additionally require the solution of nonlinear algebraic equations. On the other hand, energy-preserving methods, or methods that preserve a Lyapunov function, are not only difficult to construct but also tend to have complicated and costly implementations (see, e.g., [37]). For instance, they require solving implicit relations even in the unconstrained case. Another benefit is that geometric integrators tend to be extremely stable and can often operate with larger step sizes compared to other methods; this property is justified by the existence of a shadow Hamiltonian. Finally, from a theoretical standpoint, backward error analysis for geometric integrators tends to be simpler since it admits the same equations of motion—with slightly perturbed terms.

5 Numerical experiments

In this section we present the results of numerical experiments. Besides illustrating the feasibility of our methods, we compare to *Riemannian gradient descent* (RGD) which is a standard baseline for optimization on manifolds [2]. RGD is given by

$$q_{\ell+1} = \exp_{q_\ell}\left(-h \operatorname{grad} f(q_\ell)\right), \tag{5.1}$$

for $\ell = 0, 1, \ldots$ where $\exp_q : T_q\mathcal{Q} \to \mathcal{Q}$ is the exponential map, obtained through the geodesic flow on $\mathcal{Q}$ and is only locally defined, and $\operatorname{grad} f(q) \in T_q\mathcal{Q}$ is the Riemannian gradient of $f : \mathcal{Q} \to \mathbb{R}$ at

q, i.e., $(\operatorname{grad} f)^i(q) = g^{ij}(q)\partial f(q)/\partial q^j$ where g is the metric of $\mathcal{Q}$. To approximate the exponential map one usually needs to know a projection to the manifold $\mathcal{Q}$. When considering optimization over Lie groups or homogeneous spaces we can adapt (5.1) into the following form:

$$Y_\ell = \operatorname{Tr}\left(\partial_x f(X_\ell) \cdot X_\ell \cdot T_i\right) T_i, \tag{5.2a}$$

$$X_{\ell+1} = X_\ell \exp\left(-hY_\ell\right), \tag{5.2b}$$

where $\{T_i\}$ are the generators of the Lie algebra $\mathfrak{g}$.[5]

Let us mention some guidelines used in our experiments:

- We plot the curves for RGD, i.e., (5.1) or (5.2), as a dashed black line. The curves for our methods, (2.2) or (2.3), are shown as solid colored lines. We test a few different values of the momentum factor μ for each experiment.

- The parameters of each algorithm were tuned with a rough grid search, and in particular we choose the largest step size such that RGD attains its "best" performance. Then we use the same step size for all methods, even though (2.2) and (2.3) were often able to work with larger step sizes compared to RGD.

- We always choose $g = h$ in (2.2) and (2.3)—this was justified in [7] and corresponds to a change of variables such that discretizations of first- and second-order dynamics have the same simulation time and therefore the comparison between the associated methods is meaningful.

- For method (2.2) we use a standard root finder routine to solve the nonlinear constraint equation (2.2d); this is done with (damped) Newton's method.

5.1 Spherical spin glass

Consider the 2-spin spherical Sherrington-Kirkpatrick (SSK) model given by the Hamiltonian

$$\mathcal{H}(\sigma) = -\frac{1}{N}\sum_{i,j=1}^{N} J_{ij}\sigma^i\sigma^j - \sum_{i=1}^{N} b_i\sigma^i, \tag{5.3}$$

where $\sigma = (\sigma_1, \ldots, \sigma_N)$ is a vector on the hypersphere S^{N-1}, i.e., $\|\sigma\|^2 = N$. The disorder parameters J_{ij} and $b = (b_1, \ldots, b_N)$ are a random matrix and a random vector, respectively (they will be specified shortly). The vector b represents an external magnetic field. The SSK is a continuous approximation of a spin glass and is an important model in the theory of disordered systems, having also many applications ranging from physics to computer science. We want to find ground states,

$$\min_{\sigma \in S_{N-1}} \mathcal{H}(\sigma), \tag{5.4}$$

---

[5] For a practical implementation we actually do not need to use the generators but rather a projection to the Lie algebra:
$$\operatorname{Tr}\left(\partial_x f(X_\ell) \cdot X_\ell \cdot T_i\right) T_i = [\partial_X f(X_\ell) \cdot X_\ell]^T - \partial_X f(X_\ell) \cdot X_\ell.$$
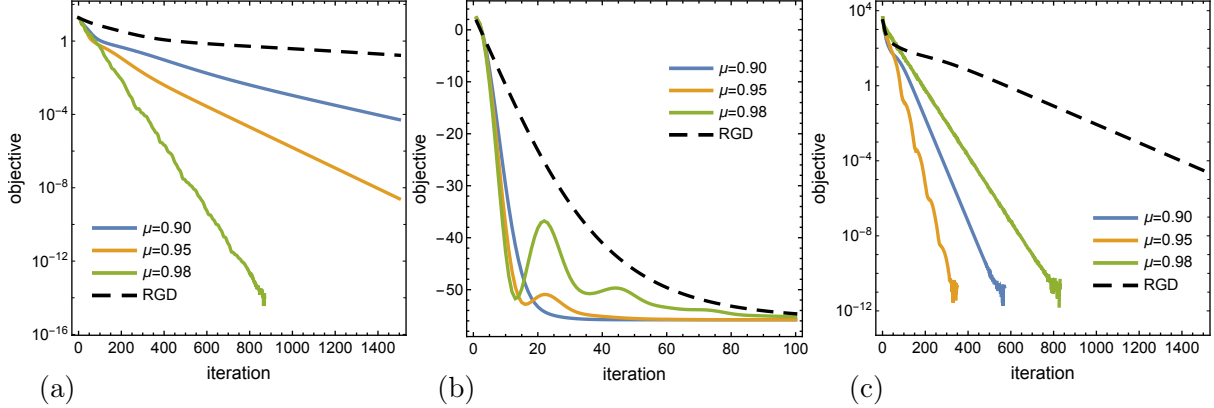We also employ this formula in our method (2.3).

Figure 2: Minimizing the SSK Hamiltonian over a sphere. We use algorithm (2.2) (with $g = hI$) and different values of μ and compare with RGD (5.1) (dashed line). We use the same step size $h = 1/L = 1/\lambda_{\max}(J)$ for both. *(a)* $J_{ij} = J_{ji} \sim \mathcal{N}(0,1)$, $J_{ii} = 0$, $b_i = 0$, and $N = 100$. In this case the exact solution is known to be $f^\star = -\lambda_{\max}(J)$. Thus the y-axis represents $f(q) - f^\star$ (in log scale). *(b)* Same setting as in *(a)* except that we add an external field $b_i \sim 0.5\mathcal{N}(0,1)$. In this case the exact solution is unknown and we plot $f(q)$. *(c)* $J = (1/n)BB^T$ where $B \in \mathbb{R}^{n \times d}$ ($n = 1000$, $d = 1100$) with entries iid from $\mathcal{N}(0,1)$ and $b_i = 0$, and minimize over the unit sphere $\|\sigma\|^2 = 1$. This problem has large condition number and is "difficult." Here we keep the step size $h = 0.05$.

using our method (2.2)—thus $\mathcal{H}$ plays the role of f and σ of the variable q. This is a particular instance of a quadratically constrained quadratic program, which in general is nonconvex and even NP hard. Problem (5.4) can, however, be solved efficiently despite its nonconvexity. In Fig. 2 we illustrate the performance of algorithm (2.2) in comparison to RGD (5.1) for few different instances of problem (5.4). We see that it significantly outperforms RGD—the constraints are satisfied to high accuracy, $\psi(\sigma) = \|\sigma\|^2 - N \approx 10^{-12}$.

5.2 Frobenius distance minimization on $SO(n)$

Consider the following matrix distance minimization problem over the rotation group $SO(n)$:

$$\min_{X \in SO(n)} \|A - X\|_F^2. \tag{5.5}$$

This is known as Wahba's problem [38] and consists in finding the best rotation matrices between two coordinate systems. Wahba's problem is also a generalization of the well-known Procrustes problem which is widespread in machine learning and statistics. Problem (5.5) is known to have an exact solution given by $X^\star = UDV^T$ where $A = U\Sigma V^T$ is the singular value decomposition of A and D is a diagonal matrix, $D_{ij} = 0$ for $j \neq i$, with $D_{ii} = 1$ for $i = 1, \ldots, n-1$ and $D_{nn} = \det(UV)$. We consider solving a few instances of problem (5.5) using our method (2.3) which performs optimization over a Lie group; we compare this method with RGD (5.2). The results are shown in Fig. 3. In Fig. 3c we slightly increased the step size, and we see that RGD became unstable, while our method remained stable. In Fig. 4 we consider a harder situation in 500 dimensions.
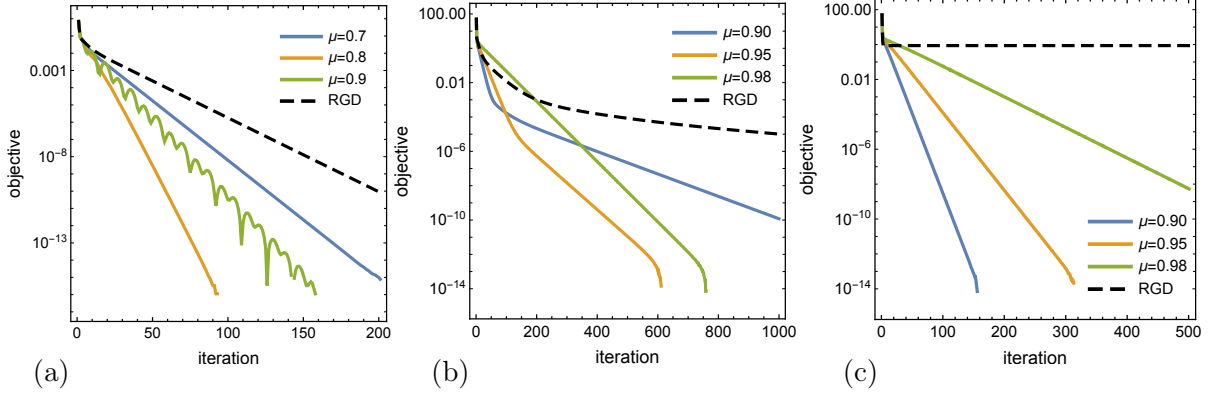
17

Figure 3: Solving Wahba's problem (5.5) with methods (2.3) and (5.2). We plot $f(X_\ell) - f(X^\star)$ since the exact solution is known. *(a)* A is a 3×3 matrix with entries sampled uniformly, $A_{ij} \sim \mathcal{U}([0, 1])$. Both methods use step size $h = 0.1$. *(b)* Higher dimensions, $n = 100$, and $A_{ij} \sim \mathcal{N}(0, 1)$. Step size is $h = 0.01$. *(c)* Same as *(b)* but with step size $h = 0.1$; here RGD became unstable.
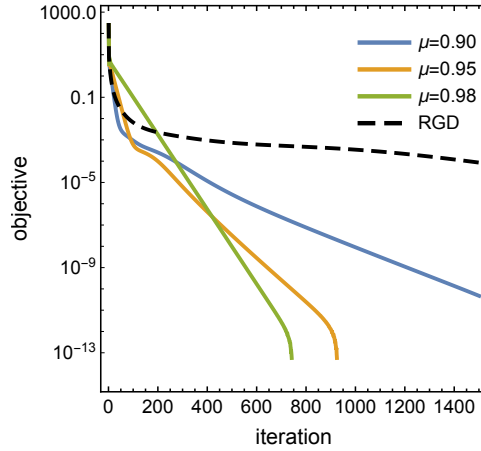

Figure 4: Solving (5.5) where $A \in \mathbb{R}^{500 \times 500} \sim \mathcal{N}(0, 1)$; $h = 0.01$ for both methods.

5.3 Maximizing alignment between vectors

Given N pairs of n-dimensional vectors, $\{(u_i, v_i)\}_{i=1}^N$, the goal is to find a single rotation matrix $X \in SO(n)$ which makes them as parallel as possible. We can do this by solving the following optimization problem (here i denotes the label of a vector and not its ith component):

$$\max_{X \in SO(n)} \sum_{i=1}^N \left(u_i^T X v_i \right)^2 . \tag{5.6}$$

We consider first a case in $\mathbb{R}^3$ as illustrated in Fig. 5. The initial and final vectors are

$$u_1 = (1.02, 0.52, 3.86)^T, \qquad u_2 = (1.61, -2.92, 0.47)^T, \qquad u_3 = (5.03, 6.21, 5.09)^T, \tag{5.7a}$$

$$v_1 = (3.21, 1.21, 4.25)^T, \qquad v_2 = (2.66, 1.08, -4.53)^T, \qquad v_3 = (-3.02, 1.60, 4.00)^T, \tag{5.7b}$$

$$\tilde{v}_1 = (-0.35, -0.70, 5.41)^T, \qquad \tilde{v}_2 = (-0.15, -4.81, -2.37)^T, \qquad \tilde{v}_3 = (2.72, 3.82, 2.39)^T. \tag{5.7c}$$
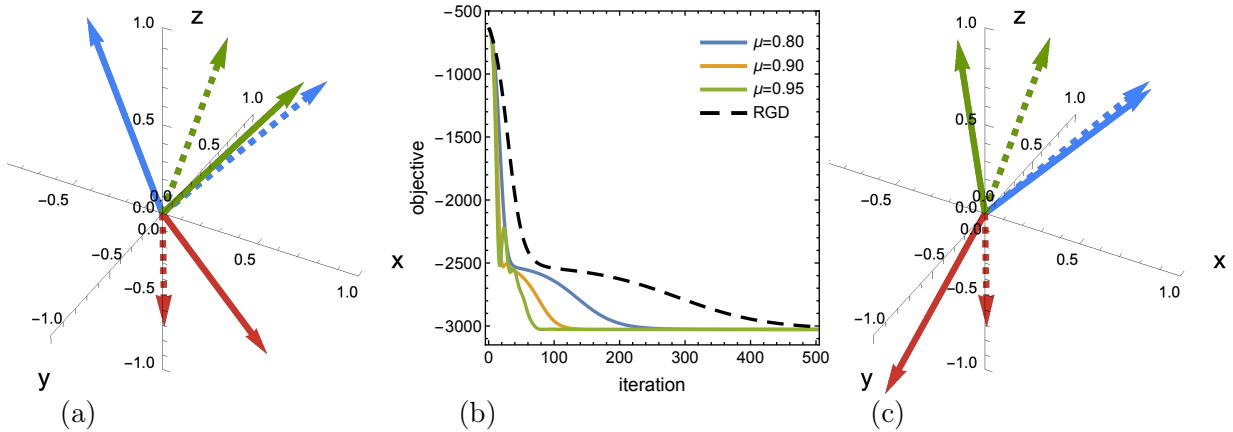
18

Figure 5: Solving problem (5.6) in $n = 3$ dimensions with $N = 3$ pairs of vectors (matching colors) whose entries are sampled from $\mathcal{N}(1, 3)$; the u_i's (v_i's) are in dashed (solid) lines. The initial configuration is shown in *(a)*; we normalize the vectors for visualization. The plot in *(b)* shows the convergence of methods (2.3) and (5.2) with step size $h = 10^{-5}$ (this was tuned so that all methods converged). The final configuration is shown in *(c)*. Note how the v_i's were rotated (the u_i's represented by dashed lines remained the same).

Here $\tilde{v}_i \equiv X^\star v_i$ where $X^\star$ is a solution of (5.6). Note how the solution obtained by (2.3) converged much faster than RGD (5.2); see Fig. 5b. In Fig. 5a and Fig. 5c we show the initial and final vectors, respectively; the u_i's are in dashed lines with their associated pairs v_i's and $\tilde{v}_i$'s in solid lines and with the same color. Let us also show their alignment by computing the vectors α and $\tilde{\alpha}$ defined as

$$\alpha_i \equiv \frac{|u_i \cdot v_i|}{\|u_i\|\|v_i\|}, \qquad \tilde{\alpha}_i \equiv \frac{|u_i \cdot \tilde{v}_i|}{\|u_i\|\|\tilde{v}_i\|} \qquad (i = 1, \dots, N). \tag{5.8}$$

Thus for this example we obtain

$$\alpha = (0.92, 0.055, 0.30)^T, \qquad \tilde{\alpha} = (0.91, 0.70, 0.99)^T. \tag{5.9}$$

Note how the second and third pairs are much better aligned which corresponds to the red and blue vectors in Fig. 5 (green corresponds to the first pair).

In Fig. 6 and Fig. 7 we consider this problem in higher dimensions. Note that since an $n \times n$ rotation matrix has $n(n-1)/2$ degrees of freedom, the problem becomes underdetermined when $N > (n-1)/2$. We can see that once again the method (2.3) clearly outperforms RGD.

5.4   Spherical spin glass via Lie group

We consider the same problem as in Sec. 5.1 but using the Lie group method (2.3), which simulates a dissipative geodesic flow over $SO(n)$. Thus, we reformulate problem (5.4) on the oriented sphere $SO(n)/SO(n-1)$:

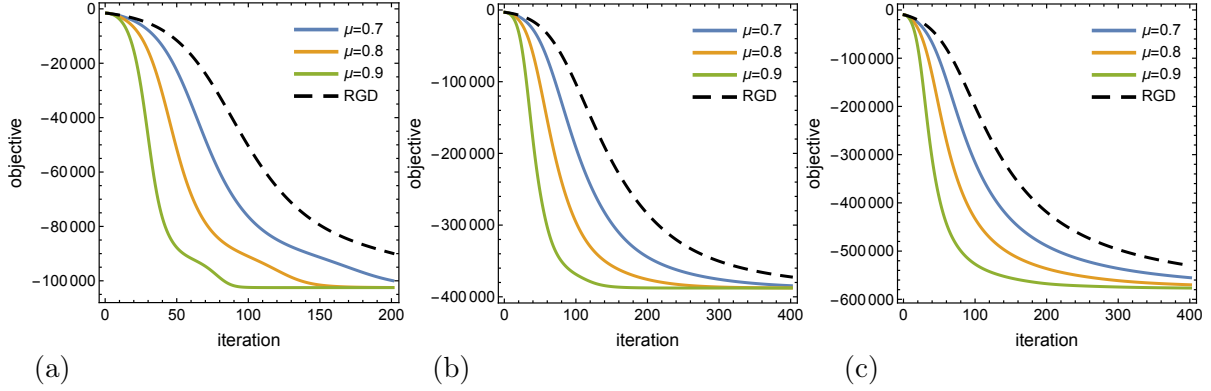$$\max_{X \in SO(n)} \frac{1}{n} \sum_{j,k=1}^{n} X_{j1} J_{jk} X_{k1}, \tag{5.10}$$

19

Figure 6: Solving problem (5.6) in $n = 100$ dimensions. We choose step size $h = 10^{-6}$ for all cases and methods. The vectors (u_i, v_i)'s are sampled from $\mathcal{N}(0, 1)$. *(a)* $N = 10$ vectors. The alignments (5.8) are shown in Fig. 7a. *(b)* $N = 49$ (see Fig. 7b). *(c)* $N = 100$ (see Fig. 7c).
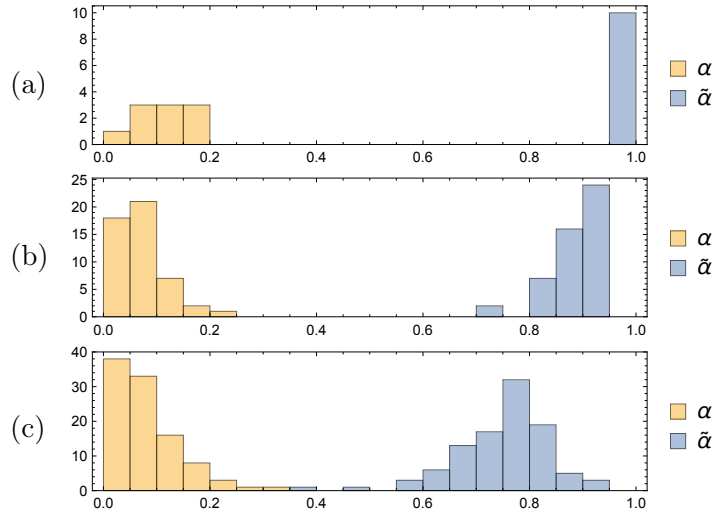

Figure 7: For the three respective cases of Fig. 6 we show histograms of the components of the vectors (5.8) which characterize the alignments; α denotes the initial alignment and $\tilde{\alpha}$ the final alignment after a solution of (5.6) is obtained. Note how the problem becomes harder with increasing N.

where J is a symmetric matrix with entries sampled from the standard normal, $\mathcal{N}(0, 1)$, and with zero diagonal elements, $J_{ii} = 0$—here we do not consider an external field b. A simulation with $n = 100$ is shown in Fig. 8. Note that this approach requires less iterations than in Fig. 2; however the computations involve several matrix multiplications besides approximating matrix exponentials. In Fig. 9 we apply method (2.3) with a range of h's and μ's to analyze its convergence during a fixed number of 600 iterations. In the Appendix E we provide a comparison of the computing time between methods (2.3) and (2.2) for this problem.
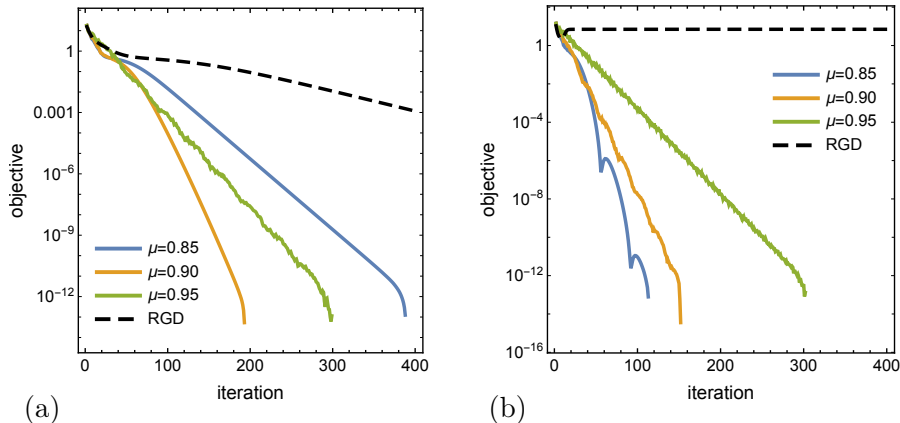
Figure 8: Solving the optimization problem (5.10)—which corresponds to the SSK model—over the homogeneous space $S^{n-1} \simeq SO(n)/SO(n-1)$ using our Lie group method (2.3). We compare with RGD (5.2). We choose $n = 100$. *(a)* $h = 0.01$ for all methods. *(b)* $h = 0.03$; RGD became unstable.
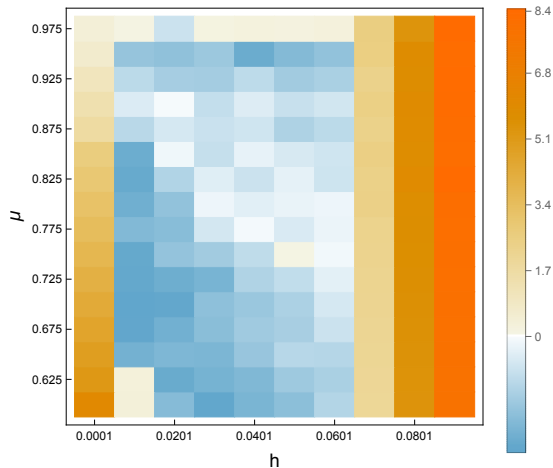

Figure 9: For similar problem as in Fig. 8 (with $n = 70$) we apply method (2.3) for a range of step sizes h and momentum factor μ. The color map indicates the difference between the objective function value (obtained with 600 iterations) minus the exact minimum. For most choice of parameters (blue and light colors) the method obtained solutions accurate up to $\approx 10^{-13}$.

6   Conclusions

We have proposed a systematic, first-principles approach to constrained optimization that leverages the well-established theory of symplectic integrators to construct "rate-matching" first-order optimization methods[6] on arbitrary smooth manifolds. To this end, we generalized symplectic ideas from conservative to dissipative settings. Central to our argument is a symplectification procedure for constrained dynamics that generalizes the recent work of [8] to the general setting of smooth manifolds.

---

[6]First-order optimization methods use only the first derivative of the objective function, i.e., gradients, as opposed to Hessians or higher-order derivatives whose computation are prohibitively expensive in high dimensions.

We have focused on the optimization problem (1.1) under equality constraints (1.2); however, the method extends in principle to inequality constraints, where $\psi_a(q) \leq 0$. The hard part of the constrained problem consists in enforcing the boundary $\psi_a(q) = 0$ since when the minimum lies in the interior region the constraints become inactive. There are subtleties, however, that may arise under the discretization that would need to be studied (cf. [39]).

Acknowledgements

References

[1] P. A. Absil, R. Mahony, and R. Sepulchre, *Optimization Algorithms on Matrix Manifolds.* Princeton University Press, 2008.

[2] H. Zhang and S. Sra, "First-order methods for geodesically convex optimization," *Conf. Learning Theory* (2016) 1617–1638.

[3] J. Townsend, N. Koep, and S. Weichwald, "Pymanopt: A python toolbox for optimization on manifolds using automatic differentiation," *J. Mach. Learn. Res.* **17** (2016) 1–5.

[4] K. Ahn and S. Sra, "From Nesterov's estimate sequence to Riemannian acceleration," *Conf. Learning Theory* (2020) 84–118.

[5] F. Alimisis, A. Orvieto, G. Becigneul, and A. Lucchi, "Momentum improves optimization on Riemannian manifolds," *Int. Conf. Artificial Intelligence and Statistics* **130** (2021) 1351–1359.

[6] A. Wibisono, A. C. Wilson, and M. I. Jordan, "A variational perspective on accelerated methods in optimization," *Proc. Nat. Acad. Sci.* **113** no. 47, (2016) E7351–E7358.

[7] G. França, J. Sulam, D. P. Robinson, and R. Vidal, "Conformal symplectic and relativistic optimization," *J. Stat. Mech.* **2020** no. 12, (2020) 124008.

[8] G. França, M. I. Jordan, and R. Vidal, "On dissipative symplectic integration with applications to gradient-based optimization," *J. Stat. Mech.* **2021** no. 4, (2021) 043402.

[9] M. Betancourt, M. I. Jordan, and A. Wilson, "On symplectic optimization," `arXiv:1802.03653 [stat.CO]`.

[10] M. Muehlebach and M. I. Jordan, "Optimization with momentum: Dynamical, control-theoretic, and symplectic perspectives," *J. Mach. Learn. Res.* **22** no. 73, (2021) 1–50.

[11] A. Bravetti, M. L. Daza-Torres, H. Flores-Arguedas, and M. Betancourt, "Optimization algorithms inspired by the geometry of dissipative systems," `arXiv:1912.02928 [math.OC]`.

[12] G. França, D. P. Robinson, and R. Vidal, "Gradient flows and proximal splitting methods: A unified view on accelerated and stochastic optimization," *Phys. Rev. E* **103** (2021) 053304.

[13] E. Hairer, C. Lubich, and G. Wanner, *Geometric Numerical Integration: Structure-Preserving Algorithms for Ordinary Differential Equations.* Springer, 2010.

[14] R. I. McLachlan and G. R. W. Quispel, "Splitting methods," *Acta Numer.* **11** (2002) 341.

[15] R. I. McLachlan, G. Quispel, and W. Reinout, "Geometric integrators for ODEs," *J. Phys. A: Math. and Gen.* **39** no. 19, (2006) 5251.

[16] B. Leimkuhler and S. Reich, *Simulating Hamiltonian Dynamics.* Cambridge University Press, 2004.

[17] J. E. Marsden and M. West, "Discrete mechanics and variational integrators," *Acta Numer.* **10** (2001) 357–514.

[18] H. C. Andersen, "Rattle: A "velocity" version of the shake algorithm for molecular dynamics calculations," *J. Comput. Phys.* **52** no. 1, (1983) 24–34.

[19] B. J. Leimkuhler and R. D. Skeel, "Symplectic numerical integrators in constrained Hamiltonian systems," *J. Comput. Phys.* **112** (1994) 117–125.

[20] S. Reich, "Symplectic integration of constrained Hamiltonian systems by composition methods," *SIAM J. Numer. Anal.* **32** no. 3, (1996) 475–491.

[21] B. Leimkuhler and C. Matthews, "Efficient molecular dynamics using geodesic integration and solvent–solute splitting," *Proc. Royal Soc. A: Math., Phys. and Eng. Sci.* **472** no. 2189, (2016) 20160138.

[22] M. M. Graham, A. H. Thiery, and A. Beskos, "Manifold Markov chain Monte Carlo methods for bayesian inference in a wide class of diffusion models," `arXiv:1912.02982 [stat.CO]`.

[23] K. X. Au, M. M. Graham, and A. H. Thiery, "Manifold lifting: scaling MCMC to the vanishing noise regime," `arXiv:2003.03950 [stat.CO]`.

[24] T. Lelièvre, M. Rousset, and G. Stoltz, "Hybrid Monte Carlo methods for sampling probability measures on submanifolds," *Numerische Mathematik* **143** no. 2, (2019) 379–421.

[25] A. Barp, A. Kennedy, and M. Girolami, "Hamiltonian Monte Carlo on symmetric and homogeneous spaces via symplectic reduction," `arXiv:1903.02699 [stat.CO]`.

[26] J. E. Marsden and T. S. Ratiu, *Introduction to Mechanics and Symmetry: A Basic Exposition of Classical Mechanical Systems.* Springer, 2010.

[27] V. I. Arnold, A. Weinstein, and K. Vogtmann, *Mathematical Methods of Classical Mechanics.* Springer, 1989.

[28] P. A. M. Dirac, "Generalized hamiltonian dynamics," *Canadian J. of Math.* **2** (1950) 129–148.

[29] P. G. Bergmann and I. Goldberg, "Dirac bracket transformations in phase space," *Phys. Rev.* **98** (1954) 531–538.

[30] P. A. M. Dirac, *Lectures on Quantum Mechanics*. Dover Publications, 2001.

[31] M. J. Gotay, J. M. Nester, and G. Hinds, "Presymplectic manifolds and the Dirac–Bergmann theory of constraints," *J. Math. Phys.* no. 19, (1978) 2388.

[32] R. I. McLachlan, K. Modin, O. Verdier, and M. Wilkins, "Geometric generalizations of SHAKE and RATTLE," *Found. Comput. Math.* no. 14, (2014) 339–370.

[33] H. Marthinsen and B. Owren, "Geometric integration of non-autonomous Hamiltonian problems," *Adv. Comput. Math.* **42** (2016) 313–332.

[34] M. Asorey, J. F. Cariñena, and L. A. Ibort, "Generalized canonical transformations for time-dependent systems," *J. Math. Phys.* **24** no. 12, (1983) 2745–2750.

[35] G. Zhong and J. E. Marsden, "Lie-Poisson Hamilton-Jacobi theory and Lie-Poisson integrators," *Phys. Lett. A* **133** no. 3, (1988) 134–139.

[36] A. C. Hansen, "A theoretical framework for backward error analysis on manifolds," *J. Geom. Mech.* **3** no. 1, (2011) 81–111.

[37] R. I. McLachlan, G. R. W. Quispel, and N. Robidoux, "Geometric integration using discrete gradients," *Phil. Trans. R. Soc. A* **357** no. 1754, (1999) 1021–1045.

[38] G. Wahba, "A least squares estimate of satellite attitude," *SIAM Review* **7** no. 3, (1965) 409–409.

[39] M. Muehlebach and M. I. Jordan, "On constraints in first-order optimization: A view from non-smooth dynamical systems," `arXiv:2107.08225 [math.OC]`.

A   A brief review of conservative Hamiltonian systems

Given a smooth n-dimensional manifold $\mathcal{M}$ we can construct its cotangent bundle $T^*\mathcal{M}$, i.e., the union of all cotangent spaces $T_x^*\mathcal{M}$ for all $x \in \mathcal{M}$, which carries a canonical symplectic structure ω.[7] Around any point $x \in \mathcal{M}$ there exists local coordinates $q = (q^1, \ldots, q^n)$ on $\mathbb{R}^n$, and we henceforth refer to x by its coordinates $q = (q^1, \ldots, q^n)$. The cotangent bundle then inherits local coordinates (q^i, p_i) around $T_x^*\mathcal{M}$ and thus can be locally identified with $\mathbb{R}^{2n}$ ($i = 1, \ldots, n$).

In such a coordinate basis we can write the 2-form[8]

$$\omega \equiv dq^i \wedge dp_i. \tag{A.1}$$

Then $(T^*\mathcal{M}, \omega)$ is a symplectic manifold.

---

[7]The cotangent space $T_x^*\mathcal{M}$ is the dual vector space to the tangent space $T_x\mathcal{M}$. It exists independently of $T_x\mathcal{M}$ and cannot be identified with it without a further (noncanonical) structure.

[8]We use Einstein's summation where repeated upper and lower indices are summed over, i.e., $u^i v_i \equiv \sum_i u^i v_i$. Also, upper indices, u^i, denote components of vectors, $u \in T\mathcal{Q}$, whereas lower indices, v_i, denote components of covectors (or dual vectors), $v \in T^*\mathcal{Q}$.

Given a function $H : T^*\mathcal{M} \to \mathbb{R}$, called Hamiltonian, ω induces a dynamical system obeying Hamilton's equations:

$$\dot{q}^i = \frac{\partial H}{\partial p_i}, \qquad \dot{p}_i = -\frac{\partial H}{\partial q^i}, \tag{A.2}$$

where $\dot{q} \equiv dq/dt$ and t denotes the time parametrization. It is immediate to check that

$$\frac{dH}{dt} = 0, \tag{A.3}$$

i.e., H is conserved along the dynamics. Hamilton's equations (A.2) can be concisely written as

$$i_{X_H}(\omega) = -dH, \tag{A.4}$$

where i_{X_H} is the interior product and X_H is the Hamiltonian vector field:

$$X_H \equiv \dot{q}^i \frac{\partial}{\partial q^i} + \dot{p}_i \frac{\partial}{\partial p_i}. \tag{A.5}$$

From (A.4), together with Cartan's formula, one can easily show that the symplectic structure is preserved, i.e., $\mathcal{L}_{X_H}\omega = 0$, where $\mathcal{L}_{X_H}$ is the Lie derivative along X_H. Conversely, one can show that any vector field X that preserves ω must locally obey (A.4) for some function H, i.e., it is, at least locally, a Hamiltonian system ($X = X_H$). This is the reason why Hamiltonian systems are special: They are the only dynamics that preserve the canonical symplectic structure of the cotangent bundle of any smooth manifold $\mathcal{M}$. *Symplectic integrators* are special discretizations because they exactly preserve this property, whose numerical trajectories can be shown to be exponentially close (in the time step) to the flow of a *shadow Hamiltonian vector field* generated by a perturbed or shadow Hamiltonian. In short, the integrator inherits all the benefits of being Hamiltonian.

We note that the fact that Hamiltonian flows evolve on $T^*\mathcal{M}$, rather than $\mathcal{M}$ as do the gradient flows, means that they are second-order dynamics that depend on two initial conditions (namely the position q and momentum p), a property that helps in the construction of *accelerated* methods for optimization [7].

B   A dissipative version of RATTLE

Following Definition 4.1, let us construct an integrator based on the well-known RATTLE method [18] for conservative systems which has been shown to be symplectic [19, 20]. We use its

general version [13] that is known to be symplectic and convergent of order $r = 2$:

$$p_{\mu,\ell+1/2} = p_{\mu,\ell} - \frac{h}{2}\left[\frac{\partial \mathscr{H}}{\partial q^\mu}(q_\ell, p_{\ell+1/2}) + \lambda_\ell^a \frac{\partial \bar\psi_a}{\partial q^\mu}(q_\ell)\right], \tag{B.1a}$$

$$q_{\ell+1}^\mu = q_\ell^\mu + \frac{h}{2}\left[\frac{\partial \mathscr{H}}{\partial p_\mu}(q_\ell, p_{\ell+1/2}) + \frac{\partial \mathscr{H}}{\partial p_\mu}(q_{\ell+1}, p_{\ell+1/2})\right], \tag{B.1b}$$

$$0 = \bar\psi_a(q_{\ell+1}) \qquad (\text{for } a = 1, \ldots, m), \tag{B.1c}$$

$$p_{\mu,\ell+1} = p_{\mu,\ell+1/2} - \frac{h}{2}\left[\frac{\partial \mathscr{H}}{\partial q^\mu}(q_{\ell+1}, p_{\ell+1/2}) + \rho_\ell^a \frac{\partial \bar\psi_a}{\partial q^\mu}(q_{\ell+1})\right], \tag{B.1d}$$

$$0 = \frac{\partial \bar\psi_a}{\partial q^\mu}(q_{\ell+1})\frac{\partial \mathscr{H}}{\partial p_\mu}(q_{\ell+1}, p_{\ell+1}) \qquad (\text{for } a = 1, \ldots, m), \tag{B.1e}$$

where $\ell = 0, 1, \ldots$ denotes the iteration number, $\mu = 0, 1, \ldots, n$ are vector components, and besides the Lagrange multipliers λ^a, which enforce the constraints (B.1c), we also have the additional Lagrange multipliers ρ^a associated to the hidden constraints required by $d\bar\psi/dt = 0$, i.e., Eq. (B.1e).[9] Recall that in the dissipative setting the constraint takes the form (3.8), however since $\alpha(q^0) > 0$ it does not affect the original constraints $\psi(q^1, \ldots, q^n) = 0$.

According to our previous construction, to obtain a method for the *nonconservative* system, all we have to do is set $q_\ell^0 = t_\ell = h\ell$ in (B.1) (and forget about p_0 since it does not enter the dynamics). Instead of considering a completely general Hamiltonian, let us particularize to the case of the geodesic Hamiltonian (3.22) which incorporates an arbitrary metric g:

$$p_{i,\ell+1/2} = p_{i,\ell} - \frac{h}{2}e^{\eta(t_\ell)}\left[\frac{e^{-2\eta(t_\ell)}}{2}\frac{\partial g^{kj}(q_\ell)}{\partial q^i}p_{k,\ell+1/2}p_{j,\ell+1/2} + \frac{\partial f(q_\ell)}{\partial q^i} + \lambda_\ell^a \frac{\partial \psi_a(q_\ell)}{\partial q^i}\right], \tag{B.2a}$$

$$t_{\ell+1} = t_\ell + h, \tag{B.2b}$$

$$q_{\ell+1}^i = q_\ell^i + \frac{h}{2}\left[e^{-\eta(t_\ell)}g^{ij}(q_\ell) + e^{-\eta(t_{\ell+1})}g^{ij}(q_{\ell+1})\right]p_{j,\ell+1/2}, \tag{B.2c}$$

$$0 = \psi_a(q_{\ell+1}) \qquad (\text{for } a = 1, \ldots, m), \tag{B.2d}$$

$$p_{i,\ell+1} = p_{i,\ell+1/2} - \frac{h}{2}e^{\eta(t_{\ell+1})}\left[\frac{e^{-2\eta(t_{\ell+1})}}{2}\frac{\partial g^{kj}(q_{\ell+1})}{\partial q^i}p_{k,\ell+1/2}p_{j,\ell+1/2}\right.$$
$$\left. + \frac{\partial f(q_{\ell+1})}{\partial q^i} + \rho_\ell^a \frac{\partial \psi_a(q_{\ell+1})}{\partial q^i}\right], \tag{B.2e}$$

$$0 = \frac{\partial \psi_a(q_{\ell+1})}{\partial q^i}g^{ij}(q_{\ell+1})p_{j,\ell+1} \qquad (\text{for } a = 1, \ldots, m). \tag{B.2f}$$

For an arbitrary metric $g(q)$ this method is implicit in the updates (B.2a) and (B.2c). However, when g is constant it becomes explicit in all updates and have a simple implementation. For the purposes of this paper, we choose g to be a constant matrix and also set the damping function to be

$$\eta(t) = \gamma t, \tag{B.3}$$

---

[9]We note that we are implicitly assuming that the Lagrange multipliers can be uniquely determined, which is guaranteed when $\partial_q\psi(\partial_{pp}\mathscr{H})\partial_q\psi^T$ is invertible—this condition is standard and also assumed for the conservative RATTLE [13].

for a constant $\gamma > 0$—other choices such as $\eta(t) = -\gamma \log t$ or a combination of these terms are also possible. Defining[10]

$$\mu \equiv e^{-\gamma h/2}, \qquad \chi \equiv \cosh(\gamma h/2), \tag{B.4}$$

and redefining the momentum as $e^{-\gamma t_\ell} p_\ell \to p_\ell$ (see [7]), the first three updates of (B.2) yield precisely the first three updates of algorithm (B.5) below. Moreover, we can replace update (B.2e) into (B.2f) and explicitly solve for the Lagrangian multipliers ρ^a, resulting in the last update (B.5d) with the projection operator defined in (2.1):

$$p_{\ell+1/2} = \mu \left[p_\ell - (h/2)\nabla f(q_\ell) - (h/2)\partial_q \psi(q_\ell)^T \lambda_\ell \right], \tag{B.5a}$$

$$q_{\ell+1} = q_\ell + h\chi g^{-1} p_{\ell+1/2}, \tag{B.5b}$$

$$0 = \psi(q_{\ell+1}), \tag{B.5c}$$

$$p_{\ell+1} = \mathcal{P}_g(q_{\ell+1}) \left[\mu p_{\ell+1/2} - (h/2)\nabla f(q_{\ell+1}) \right]. \tag{B.5d}$$

C Dissipative geodesic RATTLE

The dissipative symplectic integrator (B.5) is based on the standard RATTLE [13] and proved to be very efficient in our experiments. It is interesting to consider more efficient modern formulations of RATTLE proposed in molecular dynamics and statistics. More specifically, when the Hamiltonian is separable, it is convenient to split potential and kinetic contributions since the flow of the former can be integrated exactly, while the flow of the latter corresponds to a free geodesic motion on the constraint submanifold. Thus, consider the dissipative geodesic Hamiltonian (3.22) incorporated in the symplectification (3.7), i.e.,

$$\bar{\mathscr{H}}(q, p, \lambda, \pi) = \frac{1}{2} e^{-\eta(q^0)} g^{ij}(q) p_i p_j + e^{\eta(q^0)} f(q) + p_0 + \lambda^a \bar{\psi}_a(q), \tag{C.1}$$

where $\bar{\psi} \equiv e^{\eta(q^0)} \psi(q)$ and recall that the q dependence in g, f, ψ runs over spatial components only, i.e., $q^1, \ldots, q^n$. We now write

$$\bar{\mathscr{H}} = \bar{\mathscr{H}}_1 + \bar{\mathscr{H}}_2, \tag{C.2}$$

with

$$\bar{\mathscr{H}}_1 \equiv e^{\eta(q^0)} f(q) + e^{\eta(q^0)} \nu^a \psi_a(q), \qquad \bar{\mathscr{H}}_2 \equiv \frac{1}{2} e^{-\eta(q^0)} g^{ij} p_i p_j + p_0 + e^{\eta(q^0)} \lambda^a \psi_a(q), \tag{C.3}$$

where we introduced new multipliers for $\bar{\mathscr{H}}_1$ (the values of Lagrange multipliers are irrelevant when the constraints are satisfied). Consider the flow composition

$$e^{h\mathcal{L}_{\bar{\mathscr{H}}}} = e^{(h/2)\mathcal{L}_{\bar{\mathscr{H}}_1}} e^{h\mathcal{L}_{\bar{\mathscr{H}}_2}} e^{(h/2)\mathcal{L}_{\bar{\mathscr{H}}_1}} + \mathcal{O}(h^3), \tag{C.4}$$

where $\mathcal{L}_{\bar{\mathscr{H}}}$ denotes the Lie derivative along the flow of $\bar{\mathscr{H}}$. As will be clear shortly, the flow of $\bar{\mathscr{H}}_1$ can be integrated exactly and we can replace any second-order method to approximate the flow of $\bar{\mathscr{H}}_2$—we will use the dissipative version of RATTLE given in Eq. (B.2).

---

[10]Do not confuse this μ with the spacetime indices previously used. We use μ again for consistency with the optimization literature.

The equations of motion related to $\bar{\mathscr{H}}_1$ yield

$$\frac{dq^i}{ds} = 0, \qquad \frac{dq^0}{ds} = 0, \qquad \frac{dp_i}{ds} = e^{\eta(q^0)}\left(\frac{\partial f}{\partial q^i} + \nu^a\frac{\partial \psi}{\partial q^i}\right), \qquad 0 = \psi_a(q), \qquad \text{(C.5)}$$

where we explicitly imposed the constraints (and neglected the equation for p^0 which does not couple to the other degrees of freedom). In these equations, only p^i evolves thus the last equation is redundant if the initial position already satisfies the constraints. The original system (C.1) also satisfy the hidden constraints $d\psi_a(q)/ds = 0$ which implies

$$\frac{\partial \psi_a}{\partial q^i}g^{ij}p_j = 0. \qquad \text{(C.6)}$$

Upon differentiating this equation with respect to time once again we can solve for the Lagrange multipliers ν^a yielding

$$\frac{dp_i}{ds} = -e^{\eta(q^0)}\left[\mathcal{P}_g(q)\right]_{ij}\frac{\partial f}{\partial q^j}, \qquad \text{(C.7)}$$

where we have used the projection operator defined in Eq. (2.1). Since q^μ is constant we can integrate this equation exactly during a time interval Δs:

$$p_i(s + \Delta s) = p_i(s) - (\Delta s)e^{\eta(q^0(s))}\left[\mathcal{P}_g(q(s))\right]_{ij}\frac{\partial f(q(s))}{\partial q^j}. \qquad \text{(C.8)}$$

On the other hand, the equations of motion related to $\bar{\mathscr{H}}_2$ yield

$$\frac{dq^i}{ds} = e^{-\eta(q^0)}g^{ij}p_j, \qquad \frac{dq^0}{ds} = 1, \qquad \frac{dp_i}{ds} = -e^{\eta(q^0)}\lambda^a\frac{\partial \psi_a}{\partial q^i}, \qquad 0 = \psi_a(q). \qquad \text{(C.9)}$$

When we set $q^0 = s = t$ this corresponds to a free geodesic motion under dissipation and constraints, i.e., without the presence of an external potential. We can thus numerically solve these equations with the dissipative RATTLE (B.2)—by setting $f = 0$—which is "presymplectic" and of order $r = 2$.

Therefore, we can simply combine the exact solution (C.8) with (B.2) in approximating (C.4) within the same $\mathcal{O}(h^3)$ local error. For simplicity, let us consider the case where the metric g is constant—otherwise we just keep the implicit terms in (B.2)—to obtain

$$p_{\ell+1/2} = p_\ell - (h/2)e^{-\eta(t_\ell)}\mathcal{P}_g(q_\ell)\nabla f(q_\ell), \qquad \text{(C.10a)}$$

$$\bar{p}_{\ell+1/2} = p_{\ell+1/2} - (h/2)e^{\eta(t_\ell)}\partial_q\psi(q_\ell)^T\lambda_\ell, \qquad \text{(C.10b)}$$

$$t_{\ell+1} = t_\ell + h, \qquad \text{(C.10c)}$$

$$q_{\ell+1} = q_\ell + (h/2)\left[e^{-\eta(t_\ell)} + e^{-\eta(t_{\ell+1})}\right]g^{-1}\bar{p}_{\ell+1/2}, \qquad \text{(C.10d)}$$

$$0 = \psi(q_{\ell+1}), \qquad \text{(C.10e)}$$

$$\bar{p}_{\ell+1} = \bar{p}_{\ell+1/2} - (h/2)\partial_q\psi(q_{\ell+1})^T\rho_\ell, \qquad \text{(C.10f)}$$

$$0 = \partial_q\psi(q_{\ell+1})g^{-1}\bar{p}_{\ell+1}, \qquad \text{(C.10g)}$$

$$p_{\ell+1} = \bar{p}_{\ell+1} - (h/2)e^{-\eta(t_{\ell+1})}\mathcal{P}_g(q_{\ell+1})\nabla f(q_{\ell+1}). \qquad \text{(C.10h)}$$

28

We can further replace (C.10f) into (C.10g) and solve for ρ_ℓ, resulting into $\bar{p}_{\ell+1} = \mathcal{P}_g(q_{\ell+1})\bar{p}_{\ell+1/2}$, which can be directly combined with (C.10h) to obtain

$$p_{\ell+1} = \mathcal{P}_g(q_{\ell+1})\big[\bar{p}_{\ell+1/2} - (h/2)e^{-\eta(t_{\ell+1})}\nabla f(q_{\ell+1})\big]. \tag{C.11}$$

Now, specializing to the case of a constant damping (B.3)—one can consider analogous procedure for a general $\eta(t)$—using (B.4), and introducing the change of variable $e^{-\gamma t_\ell}p_\ell \to p_\ell$, we finally obtain the method:

$$p_{\ell+1/2} = \mu\,\mathcal{P}_g(q_\ell)\big[p_\ell - (h/2)\nabla f(q_\ell)\big], \tag{C.12a}$$

$$\bar{p}_{\ell+1/2} = p_{\ell+1/2} - (h\mu/2)\partial_q\psi(q_\ell)^T\lambda_\ell, \tag{C.12b}$$

$$q_{\ell+1} = q_\ell + h\chi g^{-1}\bar{p}_{\ell+1/2}, \tag{C.12c}$$

$$0 = \psi(q_{\ell+1}), \tag{C.12d}$$

$$p_{\ell+1} = \mathcal{P}_g(q_{\ell+1})\big[\mu\bar{p}_{\ell+1/2} - (h/2)\nabla f(q_{\ell+1})\big]. \tag{C.12e}$$

The main benefit of this formulation compared to (B.5) is that the nonlinear equation (C.12d) is more easily satisfied since the projection in (C.12a) ensures the initial momentum $p_{\ell+1/2}$ lies in the cotangent bundle of the manifold, and thus helps to ensure that $q_{\ell+1}$ stays close to the manifold; we have verified this feature numerically. Moreover, as previously mentioned, the component related to the potential $\nabla f(q)$ is integrated exactly in (C.12a) and (C.12e).

Finally, let us mention that another way to improve classical RATTLE is to note that it is only time-reversible for "sufficiently small" time steps, and it turns out that in practice this time reversibility is often not satisfied. Adding a reversibility-check update, as proposed in [24], turns RATTLE into a better behaved time-reversible integrator.

D Methods over Lie groups

A dissipative flow over a Lie group can be described by the time-dependent Hamiltonian[11]

$$H(t, X, Y) = -\frac{1}{4g}e^{-\eta(t)}\operatorname{Tr}(Y^2) + e^{\eta(t)}f(X), \tag{D.1}$$

where here $g > 0$ is a constant, $X \in \mathcal{G}$ (Lie group), and $Y \in \mathfrak{g}$ (Lie algebra). Note that X and Y are dynamical variables that evolve in time. The equations of motion over the (matrix) Lie group are given by

$$\frac{dX}{dt} = g^{-1}e^{-\eta(t)}X(t)Y(t), \qquad \frac{dY}{dt} = -e^{\eta(t)}\operatorname{Tr}(\partial_X f(X(t)) \cdot X(t) \cdot T_i)T_i, \tag{D.2}$$

where $\{T_i\}$ are the generators of the Lie algebra $\mathfrak{g}$. The presymplectic Euler method for this case corresponds to (see [8])

$$Y_{\ell+1} = Y_\ell - he^{\eta(t_\ell)}\operatorname{Tr}\left(\partial_X f(X_\ell) \cdot X_\ell \cdot T_i\right)T_i, \tag{D.3a}$$

$$t_{\ell+1} = t_\ell + h, \tag{D.3b}$$

$$X_{\ell+1} = X_\ell \exp\left(hg^{-1}e^{-\eta(t_\ell)}Y_{\ell+1}\right). \tag{D.3c}$$

---

[11]The 1/4 factor in the kinetic energy is because we do not normalize the basis of the Lie algebra to have unit norm.

On the other hand, its adjoint version—which can be obtained by running (D.3) backwards, i.e., interchanging $X_{\ell+1} \leftrightarrow X_\ell$, $t_{\ell+1} \leftrightarrow t_\ell$, $Y_{\ell+1} \leftrightarrow Y_\ell$ and $h \to -h$—is given by

$$t_{\ell+1} = t_\ell + h, \tag{D.4a}$$

$$X_{\ell+1} = X_\ell \exp\left(hg^{-1}e^{-\eta(t_{\ell+1})}Y_\ell\right), \tag{D.4b}$$

$$Y_{\ell+1} = Y_\ell - he^{\eta(t_{\ell+1})}\operatorname{Tr}\left(\partial_X f(X_{\ell+1}) \cdot X_{\ell+1} \cdot T_i\right)T_i. \tag{D.4c}$$

Now composing (D.3) with (D.4) allows us to construct a method of order $r = 2$ since the resulting method is symmetric. Also, since both methods are "presymplectic" so is their composition. Thus using the output of (D.3) evolved by $h/2$ into (D.4) that also evolves for $h/2$ yield

$$Y_{\ell+1/2} = Y_\ell - (h/2)e^{\eta(t_\ell)}\operatorname{Tr}\left(\partial_X f(X_\ell) \cdot X_\ell \cdot T_i\right)T_i, \tag{D.5a}$$

$$t_{\ell+1} = t_\ell + h, \tag{D.5b}$$

$$X_{\ell+1} = X_\ell \exp\left[(hg^{-1}/2)\left(e^{-\eta(t_\ell)} + e^{-\eta(t_{\ell+1})}\right)Y_{\ell+1/2}\right], \tag{D.5c}$$

$$Y_{\ell+1} = Y_{\ell+1/2} - (h/2)e^{\eta(t_{\ell+1})}\operatorname{Tr}\left(\partial_X f(X_{\ell+1}) \cdot X_{\ell+1} \cdot T_i\right)T_i. \tag{D.5d}$$

In the case of a constant damping (B.3), and redefining the momentum $Y_\ell e^{-\eta(t_\ell)} \to Y_\ell$, we obtain precisely the method (2.3), where we recall that μ and χ are defined in (B.4).

E   Constrained versus Lie group for SSK

We compare the formulations (5.4) and (5.10) when finding ground states of the SSK model. We thus run both methods (2.2) and (2.3) with a fixed $\mu = 0.9$. For each method we choose the largest possible step size h such that it was able to converge. Each method iterates until reaching a solution that is accurate up to $\approx 10^{-8}$. Then we measure the computation time (in seconds) for each simulation. The results are shown in Fig. 10 for three different instances of the matrix $J \in \mathbb{R}^{n \times n}$. Recall that (2.2) acts on $\mathbb{R}^n$ and all variables are vectors, while (2.3) implements the flow over the group and all variables are matrices. For the case in Fig. 10a the method (2.2) was faster, while the opposite happened in Fig. 10b. However, for larger problems both methods eventually match the computation time as shown in Fig. 10c. Note that (2.2) was able to use much larger step sizes compared to (2.3) (we do not know if this is a general feature or is particular to this problem). In particular, we observed that we could choose larger step sizes with increasing n for method (2.2), whereas the opposite happened for (2.3), i.e., smaller step sizes with increasing n was required. We should also emphasize that neither implementation was tuned for speed or scalability, i.e., there is much room for improvement in speeding up the solver for the nonlinear equation in (2.2d) as well as the matrix computations of (2.3).

F   Alternative argument for rate matching

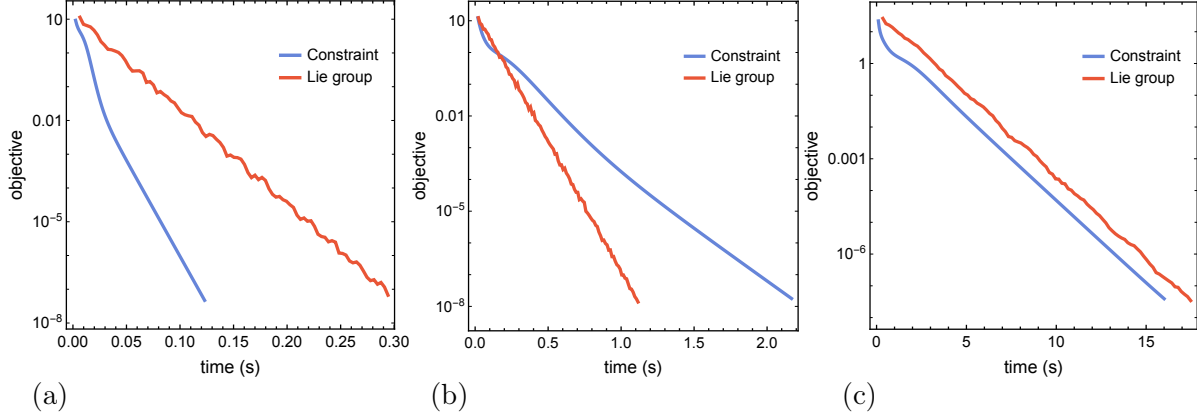We provide an alternative argument to the proof of Corollary 4.3.

Figure 10: Comparing the computation time between the method (2.2) that explicitly enforces the constraints—applied to problem (5.4)—with the Lie group method (2.3) that simulates a geodesic flow on the group—applied to problem (5.10). *(a) J* is of dimension $n = 50$. The maximum step size for (2.2) and (2.3) are $h_1 = 3$ and $h_2 = 0.03$, respectively. *(b)* Same simulation with $n = 100$, $h_1 = 5$, and $h_2 = 0.05$. *(c)* $n = 400$, $h_1 = 11$, and $h_2 = 0.02$.

Consider the Hamiltonian (3.7) over $T^*\bar{\mathcal{M}}$ which is a symplectic manifold. Using (3.6) for the specific Hamiltonian (3.22) we have that for a symplectic integrator $\Psi_h : T^*\bar{\mathcal{M}} \to T^*\bar{\mathcal{M}}$—where here we can actually assume that $\bar{\mathcal{M}} = \mathbb{R}^n$—it holds that

$$f(q_\ell) - f(q(t_\ell)) + \lambda_\ell^a \psi_a(q_\ell) - \lambda^a(t_\ell)\psi_a(q(t_\ell))$$
$$= (1/2)e^{-2\eta(t_\ell)} \left[T(q(t_\ell), p(t_\ell)) - T(q_\ell, p_\ell) \right] + \mathcal{O}\left(e^{-\eta(t_\ell)}h^r\right), \quad \text{(F.1)}$$

where $T(q,p) \equiv p \cdot g^{-1}(q)p$ is the kinetic energy. Above, we have explicitly replaced $q^0 = t$ and used the fact that the numerical method integrates q^0 and p_0 exactly. Moreover, we denote the numerical trajectories by (q_ℓ, p_ℓ). Now $\psi_a(q(t_\ell)) = 0$ identically since the constraints are satisfied by the true flow. Due to the smoothnes of a Riemannian metric we have the Lipschitz condition

$$|T(q(t_\ell), p(t_\ell)) - T(q_\ell, p_\ell)| \le L_T \left\| \begin{pmatrix} q_\ell \\ p_\ell \end{pmatrix} - \begin{pmatrix} q(t_\ell) \\ p(t_\ell) \end{pmatrix} \right\|$$
$$\le L_T C (e^{L_\phi t_\ell} - 1)h^r, \quad \text{(F.2)}$$

where we used a general upper bound on the numerical integrator, assumed to have a Lipschitz constant L_ϕ [13] (i.e., (4.12) with (4.13) in $\mathbb{R}^{2n}$). Hence

$$|f(q_\ell) - f(q(t_\ell)| \le e^{-\eta(t_\ell)}h^r \left[L_T(C/2)(e^{L_\phi t_\ell} - 1)e^{-\eta(t_\ell)} + K \right] + |\lambda_\ell^a \psi_a(q_\ell)|. \quad \text{(F.3)}$$

The numerical integrator is constructed in such a way that it remains on the same manifold as the continuous system, thus $\psi_a(q_\ell) = 0$. Note however that actually only a weaker notion would be necessary to finish the argument, i.e., that the numerical integrator satisfy the constraints to high accuracy: $|\psi_a(q_\ell)| = \mathcal{O}\left(h^r e^{-\eta(t_\ell)}\right)$. Therefore, provided the system is damped in such a way that $e^{L_\phi t_\ell - \eta(t_\ell)}$ is bounded, we conclude that

$$f(q_\ell) = f(q(t_\ell)) + \mathcal{O}\left(h^r e^{-\eta(t_\ell)}\right). \quad \text{(F.4)}$$

31